

17206

STUDIES OF NEMATIC LIQUID CRYSTALS
USING THE EPR TECHNIQUE

by

MARIJAN MARUSIC

A THESIS SUBMITTED IN PARTIAL FULFILMENT OF
THE REQUIREMENTS FOR THE DEGREE OF
DOCTOR OF PHILOSOPHY

in the Department

of

Physics

We accept this thesis as conforming to the
required standard

THE UNIVERSITY OF BRITISH COLUMBIA

July 1973.

In presenting this thesis in partial fulfilment of the requirements for an advanced degree at the University of British Columbia, I agree that the Library shall make it freely available for reference and study.

I further agree that permission for extensive copying of this thesis for scholarly purposes may be granted by the Head of my Department or by his representatives. It is understood that copying or publication of this thesis for financial gain shall not be allowed without my written permission.

Department of Physics

The University of British Columbia
Vancouver 8, Canada

Date Sept 21, 1973

ABSTRACT

The temperature dependence of the hyperfine splittings and widths of the absorption lines of two different paramagnetic probes dissolved in two nematic liquid crystals with different viscosities are studied using the EPR technique. Special attention is devoted to the changes of the hyperfine splittings and linewidths in the vicinity of the isotropic-nematic phase transition.

It is shown that the molecular ordering of the paramagnetic solutes begins before the actual phase transition temperature is reached.

Studies of the widths of the absorption lines indicate that molecular motions in nematic phases have different characteristics than those observed in the isotropic phases. It is found that Glarum and Marshall's model does not adequately describe the molecular motions in our nematic phase systems.

TABLE OF CONTENTS

	<u>Page</u>
Abstract	ii
Table of Contents	iii
List of Figures	v
List of Tables	vii
Acknowledgements	viii
CHAPTER 1	
1.1 General Introduction	1
1.2 Thesis Outline	3
CHAPTER 2	
2.1 General Description of Liquid Crystals	5
a) Nematic Liquid Crystals	6
b) Cholesteric Liquid Crystals	9
c) Smectic Liquid Crystals	13
2.2 Theories of Liquid Crystals	14
a) Swarm Theory	14
b) Continuum Theory	16
c) Statistical Theory of the nematic Liquid Crystal	16
2.3 Properties of Liquid Crystals Very Close to the Isotropic-liquid Crystal Phase Transition	17
CHAPTER 3	
3.1 Liquid Crystals Used in This Thesis	22
3.2 Free Radicals Used in This Thesis	24
CHAPTER 4	
4.1 EPR Technique and Heating System	27

	<u>Page</u>
4.2 Heating System	28
CHAPTER 5	
5.1 Viscosity of Nematic Liquid Crystals	31
5.2 The I-N Phase Transition Temperature of the System MBME + VACA	33
CHAPTER 6	
6.1 Magnetic Resonance in Liquid Crystals	36
6.2 The Order Parameter of Free Radicals Dissolved in the Nematic Liquid Crystals	38
CHAPTER 7	
7.1 Hyperfine Splitting and Order Parameter	46
CHAPTER 8	
ELECTRON SPIN RELAXATION IN LIQUID CRYSTALS	
8.1 Introduction	67
8.2 Dynamic Spin Hamiltonian	71
CHAPTER 9	
EXPERIMENTAL RESULTS	
9.1 The Widths of the Absorption Lines of the System HOAB + SL103	78
9.2 The widths of the Absorption Lines of the System HOAB + VACA	80
CHAPTER 10	
DISCUSSION	
10.1 Isotropic Phase of the System HOAB + VACA	86
10.2 Nematic Phase of the System HOAB + VACA	89
10.3 Conclusion	91
APPENDIX	94
REFERENCES	102

LIST OF FIGURES

	<u>Page</u>
FIGURE 2.1 Schematic representation of the nematic liquid crystal phase	10
FIGURE 2.2 Schematic representation of the cholesteric liquid crystal phase. The plane thickness is equal to the molecular thickness	12
FIGURE 2.3 Schematic representation of the smectic A liquid crystal phase	15
FIGURE 4.1 The heating system	30
FIGURE 5.1 The viscosities and transitions temperatures of MBBA, MBME and HOAB	34
FIGURE 5.2 The I-N phase transition temperature of the system MBME + VACA as a function of the time	35
FIGURE 7.1 The first derivative of the absorption lines of: a) VACA in a low viscosity liquid b) VACA in high viscosity liquid	47
FIGURE 7.2 The "powder" absorption line of a paramagnetic probe with axial symmetry	50
FIGURE 7.3 The first derivative of the absorption lines of: a) VACA in MBME (H n̄) b) VACA in MBME (H⊥n̄)	52
FIGURE 7.4 The hyperfine splitting of the VACA dissolved in the MBME as a function of the temperature	54
FIGURE 7.5 The hyperfine splitting of the SL103 dissolved in the MBME as a function of the temperature	55
FIGURE 7.6 Hyperfine splitting of the SL103 dissolved in the HOAB as a function of the temperature	57
FIGURE 7.7 The hyperfine splitting of the SL103 dissolved in the nematic phase of the HOAB as a function of the reduced temperature	59
FIGURE 7.8 The hyperfine splitting of the VACA dissolved in the HOAB as a function of the temperature	61

	<u>Page</u>
FIGURE 7.9 The order parameter of the SL103 and VACA dissolved in the HOAB nematic phase as a function of the reduced temperature	62
FIGURE 8.1 The order parameter as a function of the parameter λ	76
FIGURE 9.1 The peak to peak linewidths of the SL103 probe dissolved in HOAB as a function of the temp.	79
FIGURE 9.2a The peak to peak linewidths of the system HOAB + VACA as a function of the reduced temperature	82
FIGURE 9.2b The peak to peak linewidths of the system HOAB + VACA as a function of the reduced temperature	83
FIGURE 9.3 The coefficients A, B, and C from equation (8.1) as a function of the reduced temperature	84
FIGURES A.1 to A.5 $\Delta H_{m_I}^{(+)}$ and $\Delta H_{m_I}^{(-)}/m_I$ as functions of m_I^2	96-100

LIST OF TABLES

	<u>Page</u>
TABLE I Parameters for VACA	25

ACKNOWLEDGEMENTS

I wish to thank Dr. C. F. Schwerdtfeger, my research supervisor, for introducing me to the field of liquid crystals and for his assistance in the preparation of this thesis.

I would also like to express my gratitude to other members of my committee (Dr. M. Bloom, Dr. R. Barrie, Dr. D. Balzarini, and Dr. J. W. Bichard) for their discussions and their readiness to help in the time period leading up to the completion of the thesis. In particular, I wish to thank Dr. M. Bloom for many extremely useful discussions.

This research was supported by the National Research Council of Canada through research grant No 67-2228. The Graduate Fellowship from the University of British Columbia is gratefully acknowledged.

Lastly, I would like to thank my wife Marija for her patience and understanding.

CHAPTER 1

1.1 GENERAL INTRODUCTION

Liquid crystals were discovered by the Austrian botanist F.Reinitzer in 1888. Since then, the number of known liquid crystals has increased continually and it is now believed that out of every two hundred organic compounds at least one forms one or more liquid crystal phases. The main difference between the normal (isotropic) liquid and the liquid in a liquid crystal phase is the tendency of the liquid crystal molecules to align parallel to one another. Studies of these peculiar substances have increased immensely in recent years because of the possibility of their application in modern technology.

Magnetic resonance can supply much useful information about liquid crystal molecular ordering¹ and dynamics². Nuclear magnetic resonance provides the most direct experimental method to determine the molecular organization of a liquid crystal. Electron paramagnetic resonance on the other hand, does not reveal the liquid crystal properties as directly. EPR gives properties of a paramagnetic probe dissolved in liquid crystals. With a proper choice of the paramagnetic probe and a few reasonable assumptions, useful information regarding the organization³ and motion⁴ of the liquid crystal molecules can be obtained using the EPR technique.

According to Saupe's theory¹ of the nematic liquid crystal molecular orientation, the orientational order changes abruptly from zero to approximately 0.4 at the isotropic-nematic phase transition while in the liquid crystal phase the order parameter increases with decreasing

temperature. Part of this work will be concerned with the studies of the order parameter close to the transition temperature.

Most of the magnetic resonance experiments are done using nematic liquid crystals. In the electron paramagnetic resonance the vanadyl acetylacetonate (VACA) is the most common paramagnetic probe. This paramagnetic probe reveals the molecular ordering in low viscosity liquid crystals satisfactorily⁵. However, if the liquid crystal viscosity is high, we show in this work that one has to be very careful when interpreting the VACA spectra. We show that the hyperfine splitting does not change as expected, when going from the isotropic to the nematic phase of the high viscosity liquid crystal, after removing the effects of the overlapping of the resonance lines and the appearance of the powder spectrum.

From the widths and shapes of the absorption lines of a paramagnetic probe dissolved in a liquid crystal some information about the molecular motion can be obtained. The influence of a liquid crystal solvent on paramagnetic relaxation has been studied theoretically and experimentally^{5,6}. However, no systematic measurement of the paramagnetic probe linewidths as a function of the temperature have been performed to our present knowledge. Such an EPR study was, therefore, thought to be worthwhile.

In our work two liquid crystals are used. For the high viscosity measurements we use 4-methoxybenzylidene-4-amino- α -methyl cinnamic acid-n-propyl ester. For the low viscosity measurements we chose the 4,4'-di-n-heptoxyazoxybenzene (HOAB). Measurements of the hyperfine splitting of the VACA dissolved in the HOAB as a function of the temperature have been performed⁷. In these measurements⁷, however, no attention was given to the changes of the hyperfine splitting and of the linewidths

of the absorption lines very close to the isotropic-nematic phase transition. In this thesis special attention is devoted to the characteristics of the system in the vicinity of the isotropic-nematic phase transition.

Part of this investigation has been published elsewhere^{8,9}.

1.2 THESIS OUTLINE

Chapter 2 contains a general description of liquid crystals and a literature survey. Emphasis is placed on the properties of the nematic liquid crystals close to the isotropic-nematic phase transition.

Chapter 3 contains a brief description of the liquid crystals and paramagnetic probes used in our investigations.

Chapter 4 gives a short description of the experimental set up.

Chapter 5 is mainly comprised of the flow viscosity measurements of three liquid crystals. A short study of the changes of the transition temperature due to the vanadyl probe dissolved in one of the liquid crystals studied in this work is also presented.

Chapter 6 contains an introduction to the theory of magnetic resonance and the spin hamiltonian of the system.

Chapter 7 holds a description of the experimental results. The emphasis is placed on the hyperfine splitting as a function of the temperature. The order parameter of two paramagnetic probes dissolved in a low viscosity nematic liquid crystal is shown as a function of the reduced temperature.

Chapter 8 is concerned with theory of electron spin relaxa-

tion in liquid crystals.

Chapter 9 contains the experimental data of our linewidth measurements on two very different paramagnetic probes dissolved in the same low viscosity liquid crystal.

Finally, chapter 10 contains a discussion of the linewidths of the system HOAB + VACA and brief summary of our results and conclusions.

CHAPTER 2.

2.1 GENERAL DESCRIPTION OF LIQUID CRYSTALS

When certain solids are heated they do not pass directly into the liquid state but they adopt a structure which has properties intermediate between those of a true crystal and those of a true liquid. At a certain temperature the solid transforms into a turbid state or meso-phase which is both fluid and birefringent. The viscosity of such an intermediate state varies widely with different compounds and such liquids can either flow like normal liquids or be as viscous as a paste. Further increasing of the temperature converts the turbid state into the true isotropic liquid. As the liquid cools these changes take place in the reverse order but the liquid crystal state may be supercooled far below the melting point. These types of material are called "thermotropic liquid crystals". There is, however, another important class of compounds which form liquid crystal phases when they are dissolved in an appropriate solvent. These are called "lyotropic liquid crystals".

Liquid crystal molecules are large, elongated, relatively straight and in some cases flattened (with dimensions about 30\AA by 8\AA)¹⁰. They usually possess strong dipoles toward their centres and weak dipoles toward their ends.

Liquid crystals are the only liquids which are double refracting even when no external forces are present. Therefore, a convenient way to identify a liquid crystal is to test it for double refraction.

The basic question which may be asked about liquid crystals has not been answered. This question is, why do certain substances form

liquid crystals while others¹¹ do not. One possible explanation is that the attractions between the dipoles hold the molecules rather close to each other and this, combined with the long and straight geometry of the molecules, enhances the possibility for their parallel alignment. These forces combined with the hydrogen bonding and dispersion forces could account for the intermolecular potential responsible for forming liquid

However, it is generally believed that the nematic order is mainly due to dispersion forces.

Liquid crystals form three basic structures. The simplest is the nematic one which is turbid and has a (relatively) low viscosity. The only structural requirement of the nematic phase is that the molecules present a parallel or nearly parallel orientation within a certain volume of a liquid sample. The second liquid crystal structure is the cholesteric one, formed by many esters of cholesterol though curiously enough not by cholesterol itself. It has usually a higher viscosity than the nematic phase. Finally there is the smectic liquid crystal structure which has much in common with solids and may exist in several forms denoted by A, B, C,....

a) Nematic Liquid Crystals

The nematic phase is perhaps the most studied liquid crystal phase. The properties of the nematic phase indicate that the long molecular axes tend to be parallel or nearly parallel to one another. The molecules can move very easily in the direction parallel to the molecular orientation and they can rotate about their long axes.

The name "nematic" has its origin in a greek word which means "the tread"; nematic liquid crystals under the microscope show thin

mobile filaments. Studies have shown that the nematic liquid crystal are uniaxial positive¹⁰. The magnitude of the birefringence of a nematic liquid crystal is rather high. Its value varies with the temperature. The refractive index of the extraordinary ray decreases with rising temperature, while that of the ordinary ray increases. The optical axis coincides with the preferred direction of the long molecular axes.

Because of the thermal motions of the molecules, the molecular orientation is not completely parallel. The degree of the molecular ordering can be described by an ordering matrix which is defined by

$$S_{ij} = \frac{1}{2} \langle 3 \cos \beta_i \cos \beta_j - \delta_{ij} \rangle \quad (2.1)$$

where $\cos \beta_i$ ($\cos \beta_j$) is the direction cosine between the molecular axis "i" (j) and the direction of the external magnetic field which aligns the liquid crystal molecules. The angular bracket in equation (2.1) means an ensemble average.

The ordering matrix is symmetric and traceless¹. It can be diagonalized in an appropriate coordinate system. When referred to principal axes it reduces to two elements. For an axially symmetric molecule the equation (2.2) reduces to

$$S = \frac{1}{2} \langle 3 \cos^2 \beta - 1 \rangle \quad (2.2)$$

where β is the angle between the preferred direction and the long axis of a liquid crystal molecule.

By definition the S values range between 1 and $-\frac{1}{2}$. $S = 1$ means that the symmetry axis of a molecule is parallel to the preferred axis determined by an external force field; $S = 0$ corresponds to a random orientation of the molecular symmetry axes and $S = -\frac{1}{2}$ means that the symmetry axis of a molecule is perpendicular to the preferred direction. For example, investigations have shown that the VACA molecule is oriented by the nematic liquid crystal molecules in such a way that its symmetry axis is perpendicular to the preferred direction determined by the external magnetic field.

The highest S value observed in liquid crystals are between 0.8 and 0.9.

For magnetic resonance it is extremely important that the alignment of the liquid crystal molecules can be produced by the static magnetic field of the proper strength. There is, in general, a competition between the orientational effect of the sample holder's walls and the orientation imposed by the static magnetic field.

Some properties of nematic liquid crystals can be discussed conveniently by introducing the so called "director"¹². The director, $\vec{n}(\vec{r})$, describes the preferred orientation of molecules at a given point in the sample. The director is everywhere parallel to the preferred orientation. Therefore, for the case of axially symmetric molecules, the orientation is defined by the angle β between the symmetry axis and the director.

The orientation of the long molecular axes with respect to the static external magnetic field depends on the sign of the anisotropy in the magnetic susceptibility. The anisotropy in the magnetic susceptibility is usually positive, the magnetic field applied perpendicular to the container surface will tend to align the molecular axes parallel to the magnetic field.

A d.c. electric field of the proper strength will also orient the nematic liquid crystal molecules. The direction of the orientation depends on the sign of the dielectric anisotropy. Compounds exhibiting negative dielectric anisotropy have their molecules aligned parallel to a d.c. or a low frequency a.c. electric field. Experiments have shown that the electric field effects are more complicated than the magnetic field effects¹³. The alignment of the liquid crystal molecules cannot be explained by the dielectric anisotropy alone. Some effects can be explained by the anisotropic electrical conductivity and by the presence of ionizable impurities in liquid crystal.

Since the director of the unperturbed nematic liquid crystal varies continuously from the one position to the next, the sample is macroscopically isotropic. The fluctuations of the director are responsible for the turbid appearance of nematic liquid crystals. The characteristic time for the fluctuations of the director is of the order of 10^{-7} sec and depends on the wavelength of the fluctuations, while the characteristic time for the reorientation of individual molecules is about 10^{-11} sec¹⁴.

At the present time no general theory of the liquid crystals exists. There are several special theories, each of which explains only certain properties of liquid crystals but no theory explains the experimental data completely. In Figure 2.1 a simple arrangement of the nematic liquid crystal molecules is shown.

b) Cholesteric Liquid Crystals

The molecules in the cholesteric phase lie with their long axes parallel to one another as in the nematic phases. However, in the cholesteric phase the molecules are arranged in layers with their long

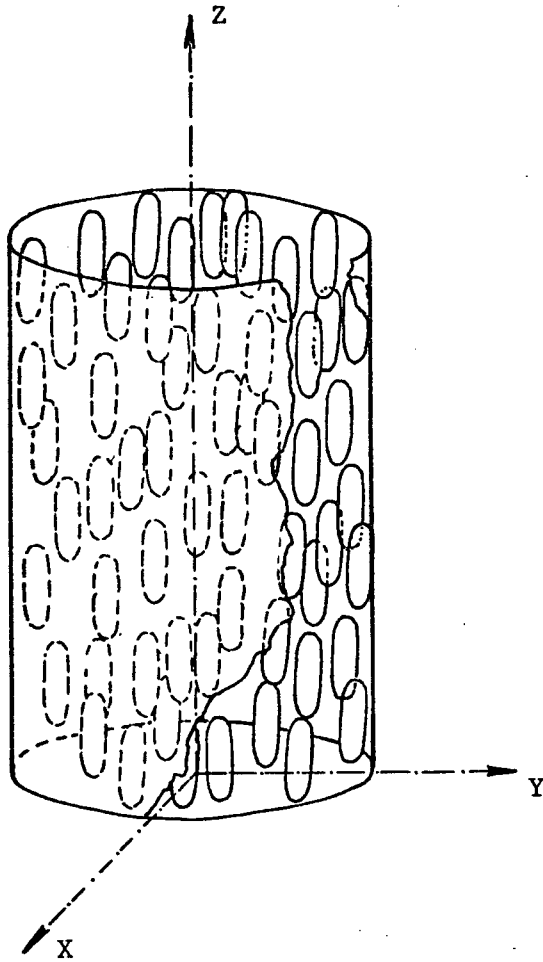


FIGURE 2.1. Schematic representation of the nematic liquid crystal phase

axes in the plane of the layer. On passing from one layer to the next the direction of the long molecular axes rotates through a constant angle. This is shown in Figure 2.2. The resulting structure is therefore akin to that of a twisted nematic liquid crystal. The cholesteric structure is optically active and presents a strong optical rotatory power. In the z-direction going from one molecular plane to the next, we can see that molecules are twisted in a helical system. The pitch of the system determines the layered character of the structure. The twist in most cholesteric liquid crystals only amounts to a rotation of about 15° between the adjacent planes. The cholesteric liquid crystal molecules are always perpendicular to the axis of the pitch.

A magnetic field changes the pitch of the helical structure when applied perpendicular to it. By increasing the magnetic field the pitch increases, until a stage is reached when the pitch becomes infinite¹⁵. At this field the cholesteric liquid crystal transform into the nematic liquid crystal. The pitch of the helix also changes as a function of the temperature, but these variations are not well understood yet.

The addition of a very small quantity of a material whose molecules do not form a cholesteric phase but are optically active to a nematic liquid crystal, causes the transformation of the nematic liquid crystal to a cholesteric one¹⁶.

It has been observed that a binary mixture of the cholesteric liquid phases which rotate the plane of polarization of light in the opposite senses, become nematic when the optical activity of mixture vanishes. Because of this and some other properties a few workers believe that the cholesteric liquid crystals are a special form of the nematic liquid crystals¹⁷.

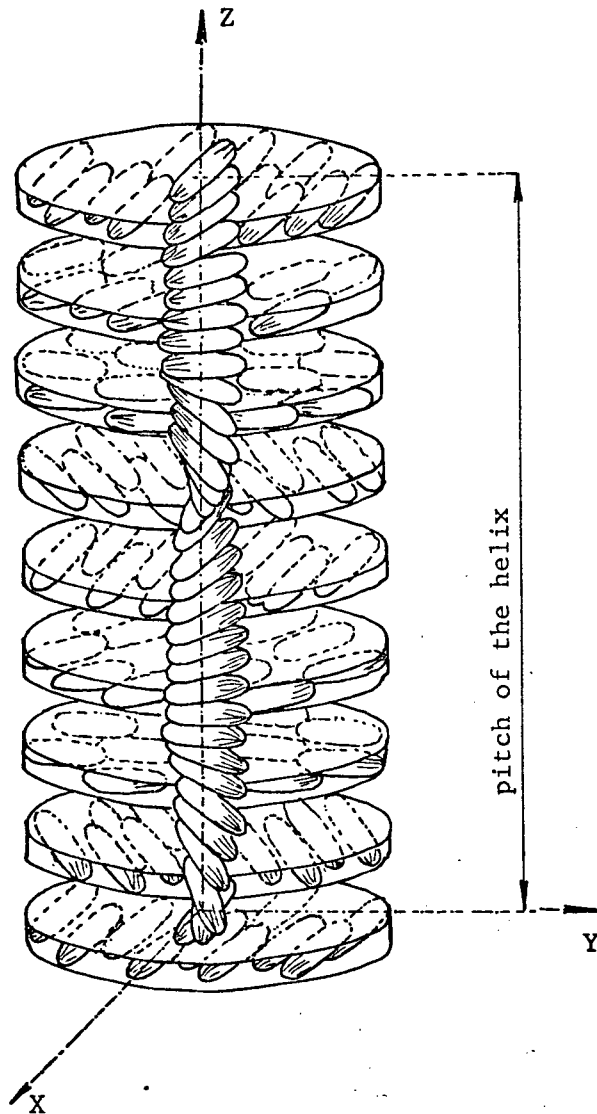


FIGURE 2.2 Schematic representation of the cholesteric liquid crystal phase. The plane thickness is equal to the molecular thickness.

c) Smectic Liquid Crystals

Smectic liquid crystals consist of the elongated molecules which are arranged in equidistant planes or layers. The thickness of such a layer is approximately the length of the molecule. The layers are flexible and would straighten out if bent. The long axes of the molecules in such a layer may be perpendicular to the layer or tilted with respect to the normal of the plane^{18,19}. The tilt angle is usually temperature dependent.

The layers in the smectic structure can slide easily with respect to one another. Clearly, a variety of molecular arrangements within a layer are possible and this has led to the characterization of smectic liquid crystals into several types. Five different smectic phases have been reported¹⁴, but the structures of only a few are known with any certainty. In the smectic A phase the preferred orientation of the molecular long axes is orthogonal to the layer. The molecules within a layer are able to rotate around their long axes and they can not move from one layer to another.

The only difference between the structure of the smectic A and C phases is that in the smectic C phase the long molecular axes are tilted with the respect to the layers. This causes the distance between the layers to be smaller than the molecular length.

The molecular centres within the layers of a smectic B liquid crystal are regularly arranged. The spatial arrangement is thought to be a hexagonally close packed one¹⁴. The molecular long axes in this phase may be either orthogonal or tilted with the respect to the smectic layers.

The molecular order is temperature independent in the smectic phase²⁰ which is in contrast to the nematic phase. The high viscosity of the smectic phase may explain this. Optically the smectic A phase is uniaxial, but the smectic C phase is biaxial²¹. Most smectic liquid crystals possess a higher temperature nematic phase.

When cooling such a liquid crystal from the nematic phase into the smectic phase in a moderate magnetic field (~ 3 kilogauss), the smectic layers orient homogeneously with the layers perpendicular to the magnetic field.

In the Figure 2.3 a simple arrangement of the smectic liquid crystal molecules is shown.

2.2 THEORIES OF LIQUID CRYSTALS

a) Swarm Theory

The Swarm theory is the oldest liquid crystal theory²². According to this theory, the liquid crystal molecules gather into groups (Swarms) of different sizes. The swarms fluctuate owing to the thermal motions, and this causes the optical axes of the swarms to oscillate. These oscillating swarms produce strong light scattering, so that a liquid crystal in the nematic phase appears milky. Each swarm contains on the average about 10^5 molecules. Within a swarm the molecules lie parallel one to another. The interactions between the swarms are weak, so that the orientation of the swarms with respect to one another is random. Moderate magnetic fields (> 2 kilogauss) can orient these swarms with their long axes parallel to the field.

This theory has been severely criticized in recent years.

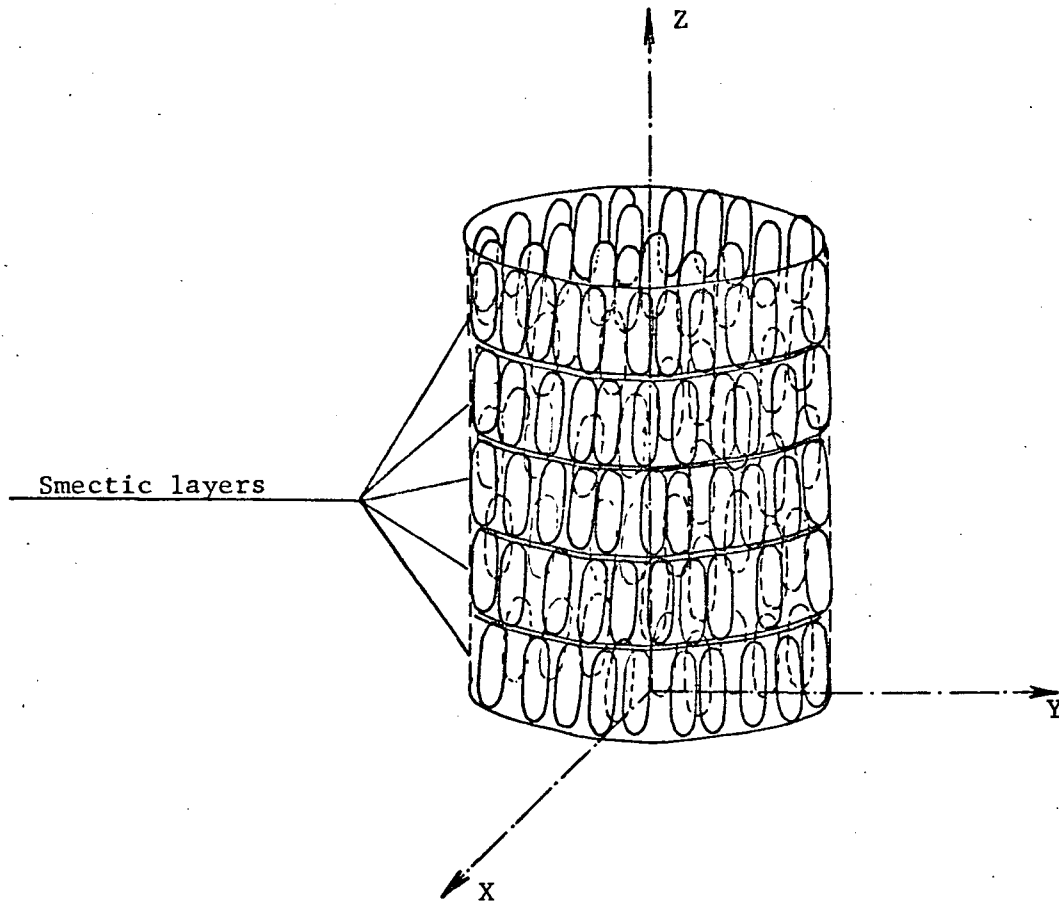


FIGURE 2.3 Schematic representation of the smectic A liquid crystal phase.

b) Continuum Theory

The so called "continuum theory" is based on the assumption that at every point in an undisturbed liquid crystal there is a definite preferred direction for the orientation of the long molecular axes. According to this theory the direction of the long molecular axes is determined by the influence of the container's walls and by external fields. The preferred direction varies continuously with position. As a consequence of this assumption, one may expect that liquid crystals have a definite structure. The elastic moduli which describe the elastic liquid crystal structure should formally be included in the elastic theory of solids. They may be ignored in solids since the ordinary elastic constants have 10^{16} greater magnitude²³.

c) Statistical Theory of the Nematic Liquid Crystals

The statistical theory proposes to describe the order-disorder transition and it attempts to predict the temperature dependence of the orientational order. According to Maier's theory^{24,25} of the nematic liquid crystals, the main reasons for the formation of a nematic state, are the dispersion forces between molecules. This theory predicts that the degree of the ordering S should be a universal function of the reduced temperature $T_R^* = \frac{T}{T_k}$, where T_k is the phase transition temperature. Experiments with different nematic liquid crystals have shown that this prediction holds reasonably well¹. To get the exact temperature dependence of the orientational order some additional terms have been introduced into Maier's expression for the intermolecular potential.

Taking into account only the dispersion forces, the potential energy of the i^{th} molecule in the field of all other molecules is

$$E_i = -\frac{A}{V^2} S \left(1 - \frac{3}{2} \sin^2 \beta_i \right) \quad (2.3)$$

where A is a characteristic of the substance and can be calculated from the transition temperature if the molar volume, V , of the nematic liquid crystal and of the isotropic liquid at the transition temperature are known.

The order parameter (the degree of the ordering) S is a measure of the long range order which exist over many thousands of molecules, when a liquid is in the nematic phase. Analyses of experimental results show that very close to the isotropic-nematic (I-N) phase transition a description using only the long-range order is not adequate²⁶, and that at these "critical temperatures" short-range order becomes more and more important.

2.3 PROPERTIES OF LIQUID CRYSTALS VERY CLOSE TO THE ISOTROPIC-LIQUID CRYSTAL PHASE TRANSITION.

Several properties of liquid crystals have been studied very close to the I-N phase transition. Hoyer and Nolle²⁷ studied the absorption and velocity of the ultrasound waves in the isotropic and nematic phases of p-azoxyanisole (PAA) and in the isotropic and cholesteric phases of cholesteryl benzoate. They found a sharp minimum in the sound velocity and a sharp maximum in the absorption of the ultrasound energy

at the phase transition temperature. The changes in the absorption energy and in the sound velocity appeared several degrees above the transition.

Several years after Hoyer and Nolle's original experiments many papers describing ultrasound experiments in liquid crystals appeared. Kapustin²⁸ studied the sound absorption in p,p'-nonoxybenzaltoluidine at frequencies from 2-15 MHz. He found that the sharpest absorption maximum occurs at the frequency 2.2 MHz. The increase in the sound velocity after its minimum had been reached was ascribed to the ordering among the molecules in the nematic phase.

Very interesting results were reported recently²⁹. Experiments with ultrasound were performed using an external magnetic field to orient the liquid crystal molecules. It was found that the orientational anisotropy of the ultrasound absorption is strongly temperature dependent in the nematic phase but no anisotropy in the sound velocity was observed. The pretransitional effects were clearly seen from the sound absorption measurements, but no such effects were detected in the velocity of the sound waves which is contradictory to the Kapustin's experiments and this has not been explained.

Optical studies of liquid crystals very close to the I-N phase transition have given very interesting information about fluctuations of the physical properties. Some physical properties were explained by the heterophase fluctuations, and some were ascribed to the changes of the size of the molecular clusters. Tsvetkov³⁰ studied the electrical birefringence (Kerr effect) of p-azoxyanisole and p-anisalaminoazobenzene at the I-N phase transitions. He concluded that changes in the birefringence are caused by the appearance of supramolecular formations in the isotropic phase, which have the same structure as the liquid crystal phase.

The time dependence of the local fluctuations of the ordering of the liquid crystal molecules in the isotropic phase has been measured by ^{31a,b} light scattering. It was found that fluctuations relax exponentially with a single relaxation time, τ , and that τ diverges as the clearing point temperature was approached from above. The relaxation time can be described by the expression

$$\tau = \frac{C}{(T - T^*)^\gamma} \quad (2.4)$$

T^* is a temperature slightly below I-N phase transition temperature, C is a constant. They found $\gamma = 1.33$. These measurements demonstrated that although the I-N phase transition is of the first-order, the liquid crystals behave over a wide temperature range as if it were going to be a second-order phase transition. These results can be adequately described by the mean-field model over most of the temperature range, but the mean-field model fails very close to the I-N phase transition. This model fails because it does not include the effects of the large fluctuations of physical properties at the I-N phase transition.

NMR (nuclear magnetic resonance) studies of the pure nematic liquid crystals and of the solutes dissolved in a nematic liquid crystal, can provide a wealth of information about the system liquid crystal-solute. The fluctuations in the orientation of the director play a strong role in the spin-lattice relaxation. The work done so far has been concerned mainly with the proton spins. The spin-lattice relaxation time is affected by the dipole-dipole interaction between nuclear spins in a molecule and these motions are modulated by the orientational modes.

Pincus³² estimated the contributions to the spin-lattice and the spin-spin relaxation times in a nematic liquid crystal arising from the fluctuations in the orientational order. For the case, when the internuclear vector is parallel to the external magnetic field, he found that the spin-lattice relaxation time, T_1 , depends on the nuclear resonance frequency: $T_1 \propto \omega^{\frac{1}{2}}$. This is in contrast to the isotropic liquids where T_1 has small frequency dependence. Doane³³ measured T_1 for PAA and for HOAB. He found poor agreement of the temperature dependence of T_1 with the Pincus' theory and their measurements indicated that the observed T_1 may be an intermolecular process rather than an intramolecular process. Recent calculations by Doane³⁴ show that the spin-lattice relaxation time is proportional to the product $\omega^{-\frac{1}{2}} S^2$, where S is the liquid crystal order parameter. This product has a very small temperature dependence which is in agreement with experiments.

Cabane et al³⁵ studied the NMR spectrum of N^{14} in the nematic and isotropic phase of PAA. In the nematic phase the N^{14} spectrum consists of four lines. In the isotropic phase the N^{14} spectrum consists of a single line. They describe the temperature dependence of the width, Δ , of this line in the isotropic phase by

$$\Delta = \frac{5.0 (^\circ K^{-\frac{1}{2}} \text{ gauss})}{(T - T^*)^{\frac{1}{2}}} \quad (2.5)$$

To understand this dependence they consider the spin relaxation in the nematic phase and then they extend it to the isotropic phase. Since the spin relaxation is proportional to the correlation length, ξ , and since by the Landau mean field theory ξ is proportional to $(T - T^*)^{-\frac{1}{2}}$ they

conclude that the linewidth has to be proportional to $(T - T^*)^{-\frac{1}{2}}$. The appearance of the temperature T^* instead of T_k was justified by the fact that the nematic-isotropic transition in PAA is weakly first-order. Cabane² has recently shown that T_1 for N^{14} at $\omega_n = 3$ MHz within the whole isotropic temperature range is proportional to $(T - T^*)^{\frac{1}{2}}$. In this paper Cabane concludes that in the isotropic phase of a nematic liquid crystal there are two types of fluctuations which can be studied with different frequencies. At a high frequency the nuclear relaxation is produced by the elastic modes similar to those of the nematic phase. The nuclear relaxation at a low frequency is dominated by the critical fluctuations of the magnitude of the local anisotropy.

Ghosh³⁶ et al have measured the proton spin-lattice relaxation time in MBBA at two frequencies in the temperature range just above I-N phase transition. They divided the experimental spin-lattice relaxation time into two parts: the relaxation time due to the critical fluctuations, and relaxation time from other sources. In their analysis they show that T_1 due to the critical fluctuations has a minimum at approximately 9°C above the I-N phase transition.

CHAPTER 3

3.1 LIQUID CRYSTALS USED IN THIS THESIS

Several liquid crystals which form the nematic phase were studied. The conclusions of this thesis are based mainly on studies of two of them:

1. 4-methoxybenzylidene-4-amino- α -methyl cinnamic acid-propyl ester (MBME)
2. 4,4'-di-n-heptoxyazoxybenzene (HOAB)

MBME liquid crystal has a melting point at $\sim 54^{\circ}\text{C}$ and an I-N phase transition at $\sim 82^{\circ}\text{C}$. The transition temperature of pure MBME changes after being heated for several hours in a vacuum at 80°C and then remains constant. It is very easy to supercool this liquid crystal to room temperature³⁷.

It has been known that the order parameter of a nematic crystal does not change much by the addition of small quantities of substances which themselves do not form mesophases. This is not true for the I-N temperature. In some cases very small quantities of impurities may change the transition temperature several degrees. For example, vanadyl acetylacetonate (VACA) changes the I-N transition temperature of MBME in a few hours by about 10 degrees (depending on the VACA concentration). This probably happens, because a slow chemical reaction between MBME and VACA takes place.

HOAB has two liquid crystal phases. Isotropic above 122°C ,

a nematic phase, between 122°C and 92°C and passes into a smectic phase between 92°C and 74°C. The viscosity of the nematic phase of HOAB is smaller than that of MBME and since it does not react with VACA, HOAB + VACA is a relatively simple system to study. Experiments described here are mainly devoted to this system. The viscosity of HOAB in its smectic phase is about 10^4 times higher than the viscosity of its nematic phase³⁸. The phase transition temperature of HOAB is not very sensitive to impurities.

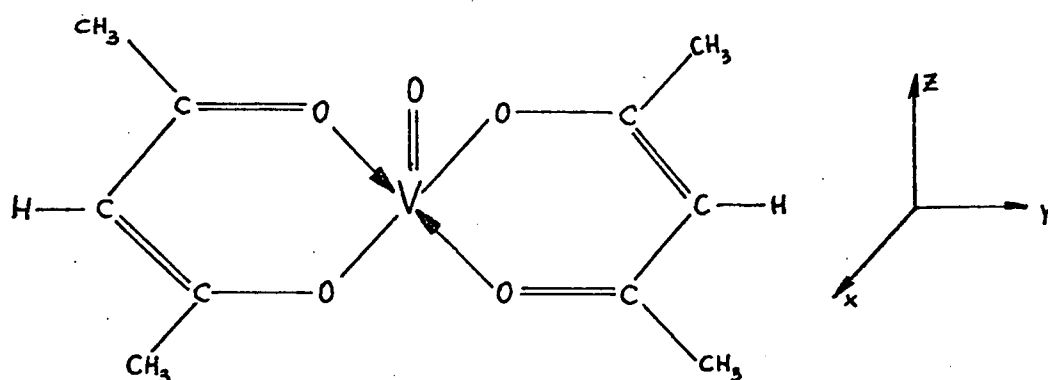
Weber³⁹ studied the temperature dependence of the second moments of the homologous series of 4,4'-alkoxyazoxybenzenes. He found that the order parameter of HOAB changes from the value 0.30 at the I-N transition temperature to the value ~ 0.55 at the nematic-smectic phase transition temperature.

Electron paramagnetic resonance (EPR) studies of the HOAB + VACA system have appeared in the literature. Gelerinter¹⁹ et al, measured the tilt angle in the smectic phase of HOAB and found it to be 30°. Šentjurc⁷ et al, measured the effects of d.c. electric fields on the order parameter as a function of the temperature. They concluded that the molecules in the smectic phase are aligned with the long molecular axes perpendicular to the d.c. electric field, whereas a d.c. electric field orients the long axis of the HOAB molecules in the nematic phase parallel to it.

3.2 FREE RADICALS USED IN THIS THESIS

Although several free radicals were used, the main conclusions are based on two of them.

The most commonly used free radical in liquid crystal studies is vanadyl acetylacetonate (VACA)



The EPR spectrum of VACA has been extensively studied and consists of eight hyperfine absorption lines. The vanadium 51 is responsible for the EPR spectrum because of its electronic spin ($S = \frac{1}{2}$) and its nuclear spin ($I = 7/2$). The V^{51} ion has a $3d^1$ configuration and since the orbital angular momentum is quenched by the crystal fields, the paramagnetism of the vanadyl ion arises from a single unpaired spin. The vanadyl oxygen is attached axially above the vanadium and the V—O bond determines the Z-axis of the system.

The electronic structure of the vanadyl ion has been studied by Ballhausen⁴⁰ et al, and later by Kivelson and Sai-Kwing Lee⁴¹. They conclude that the orbital in which the unpaired electron is found, is almost completely localized on the vanadium in the d_{xy} atomic orbital.

This orbital has a node at the nucleus and therefore the spin density should be zero at the nucleus. However, the configuration interaction or core polarization gives a ground state with a spin density which is not zero at the nucleus, thus giving a hyperfine splitting.

The VACA g-tensor and the hyperfine splitting tensor are both nearly symmetric axial in the same principal axis coordinate system. The actual magnitude of tensor components changes slightly from one solvent to the another. Values for the g-tensor and the hyperfine tensor which will be used in our calculations are given in the table I and were taken from the work of Wilson and Kivelson⁴².

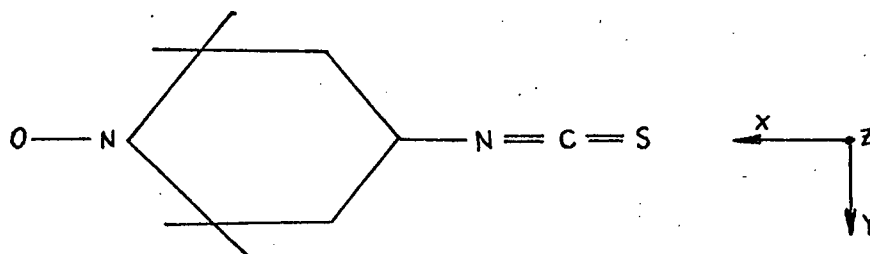
TABLE I

$g_{xx} = 1.979$	$A_{xx} = -68.0$ gauss
$g_{yy} = 1.985$	$A_{yy} = -64.0$ gauss
$g_{zz} = 1.943$	$A_{zz} = -183.0$ gauss

VACA was chosen for our studies since its spectrum is well understood, its molecule has a planar shape, and since it is relatively stable over the temperature range in which the experiments were performed.

Many studies of the molecular ordering in nematic liquid crystals have been done using VACA as a paramagnetic probe^{3,43}. The analysis of the results shows that the magnitude of the order parameter as measured by EPR is the same as that measured by optical or NMR technique on the pure liquid crystals.

Another free radical which was used was 4-isothiocyanato-2,2,6,6,-tetramethylpiperidinoxyl (SL103)



The unpaired electron is localized almost entirely on the nitrogen nucleus which has the nuclear spin $I = 1$. Therefore, the spectrum consists of three hyperfine absorption lines. It has been found that the principal axes for the g-tensor and for the hyperfine tensor lie parallel to one another. The g-tensor is not symmetric about the Z-axis, but the hyperfine tensor is approximately symmetric. The principal values for the g-tensor are $g_{xx} = 2.0089$, $g_{yy} = 2.0061$, and $g_{zz} = 2.0027$. The principal values for the hyperfine tensor are $A_{xx} \approx A_{yy} \approx 6$ gauss and $A_{zz} = 31$ gauss. The SL103 is easily soluble in all studied liquid crystals. It does not react with them, and is very stable in the studied temperature range. It will be shown later however, that SL103 is not a very good paramagnetic probe to study the order parameter of liquid crystals.

The average volume of the samples studied was $\sim 0.4\text{cm}^3$.

Free radicals were dissolved in the liquid crystals at temperatures 10 - 15°C below the I-N phase transition. These solutions of free radicals and liquid crystals were inserted into teflon holders. Although the EPR spectra were usually recorded under normal atmospheric conditions, occasionally, experiments were performed in vacuum and for these measurements the sample holders were made of pyrex glass.

CHAPTER 4

4.1 EPR TECHNIQUE AND HEATING SYSTEM

The EPR spectra were obtained with a spectrometer operating at the microwave frequency of 9.16 GHz. As a microwave power source a Varian Associate reflex klystron V - 153/6315 (max. output power 70mW), powered by a Hewlett-Packard HP 716 B power supply was employed.

From the klystron the microwaves first passed through a Microwave Associates one way ferrite isolator and a cross-arm directional coupler into a Starrett flap-attenuator. Then the microwaves entered into a magic tee bridge. The microwave power was then fed into two arms. One arm ended in a TE₁₀₂ resonance cavity, coupled through an adjustable teflon spacer. The other arm contained a slide screw tuner (De Mornay-Bonardi BGG - 459) and a matched load. Home made cavities were usually used, except for a few experiments, when the Varian multi-purpose V-4531 cavity was used. The Microwave 1N 23B crystal detector coupled the cavity signal to a preamplifier. To modulate the magnetic field and to provide the reference signal for phase sensitive detection a 100 KHz oscillator was used. The phase sensitive detector employed was a PAR (Model 121) Lock-in-amplifier. The output signal from the Lock-in-amplifier was recorded directly on a Hewlett-Packard-Moseley (Model 680) strip chart recorder.

The magnetic field was modulated through small modulation coils attached on the walls of the microwave cavity. The modulation amplitude used was between 0.1 - 6.0 gauss, for VACA typically about 3 gauss.

The Klystron frequency was stabilized by a 10 KHz modulation imposed on its reflector voltage by an Automatic Frequency Controller. The resulting microwave frequency produced a 20 KHz signal at the amplifier when the klystron was on the cavity resonance frequency. If the klystron was on either side of the resonance a 10 KHz signal of the appropriate phase was measured at the preamplifier. This signal, when amplified and rectified by a phase sensitive detection in the AFC, gave an error feed-back signal to shift the klystron frequency to the cavity resonance.

The frequency of the microwaves was measured with a digital frequency meter (Hewlett-Packard Frequency converter 5255A and an Electronic Counter 5245L).

In all experiments a Magnion magnet of range from 0 to 14 Kilo-gauss was used with a rotating coil field sensor. The magnet was powered by a Magnon 415-1365C power supply controlled with an FFC-4 field regulator. The direct reading field dials were calibrated using a glycerine NMR probe magnetometer.

4.2 HEATING SYSTEM

The temperature of the samples was measured with a Fenwall Electronic Inc. thermistor (GA 51P1) incorporated in a simple bridge. When measurements were performed with the Varian cavity the Varian nitrogen flow heating system was used. With this heating system it was not possible to control a temperature to better than $\pm 1^{\circ}\text{C}$. For the measurements very close to the phase transition temperature a special cavity and heating system were constructed. With this apparatus the temperature could be

controlled to 5 millidegree over a two hour period.

The heating system was composed of a copper sleeve about which a bifilar heating coil was wound. The resistance of the heating coil was 3.5 ohm and the coil was powered by the Kepco Operational Power Supply OPS7 - 2B, which gives d.c. current in the range 0 - 2A and voltage 0 - 7V. The output voltage was controlled between appropriate terminals. The thermistor was built into the copper block (Figure 4.1) cavity and was a part of a Wheatstone bridge and the second thermistor served as the variable feedback resistance. The cavity was mounted in the middle of the copper sleeve and both were inserted into a glass dewar for good heat insulation. The dewar vessel was properly closed to prevent air circulation. In order to change the sample temperature 0.1°C the system required ~ 30 minutes to equilibrate. The relative temperature measurements were accurate to at least 0.01°C , and the absolute temperature was determined to $\pm 1^{\circ}\text{C}$.

We believe that temperature gradients existed across our samples (length ~ 1 cm) were smaller than 0.01°C . A temperature gradient of $0.01^{\circ}\text{C}/1$ cm would broaden the absorption lines of the VACA probe by less than 1 gauss, while the lines were 40 - 60 gauss broad.

1. Wheatstone bridge
2. Null voltmeter
3. Operational Power Supply

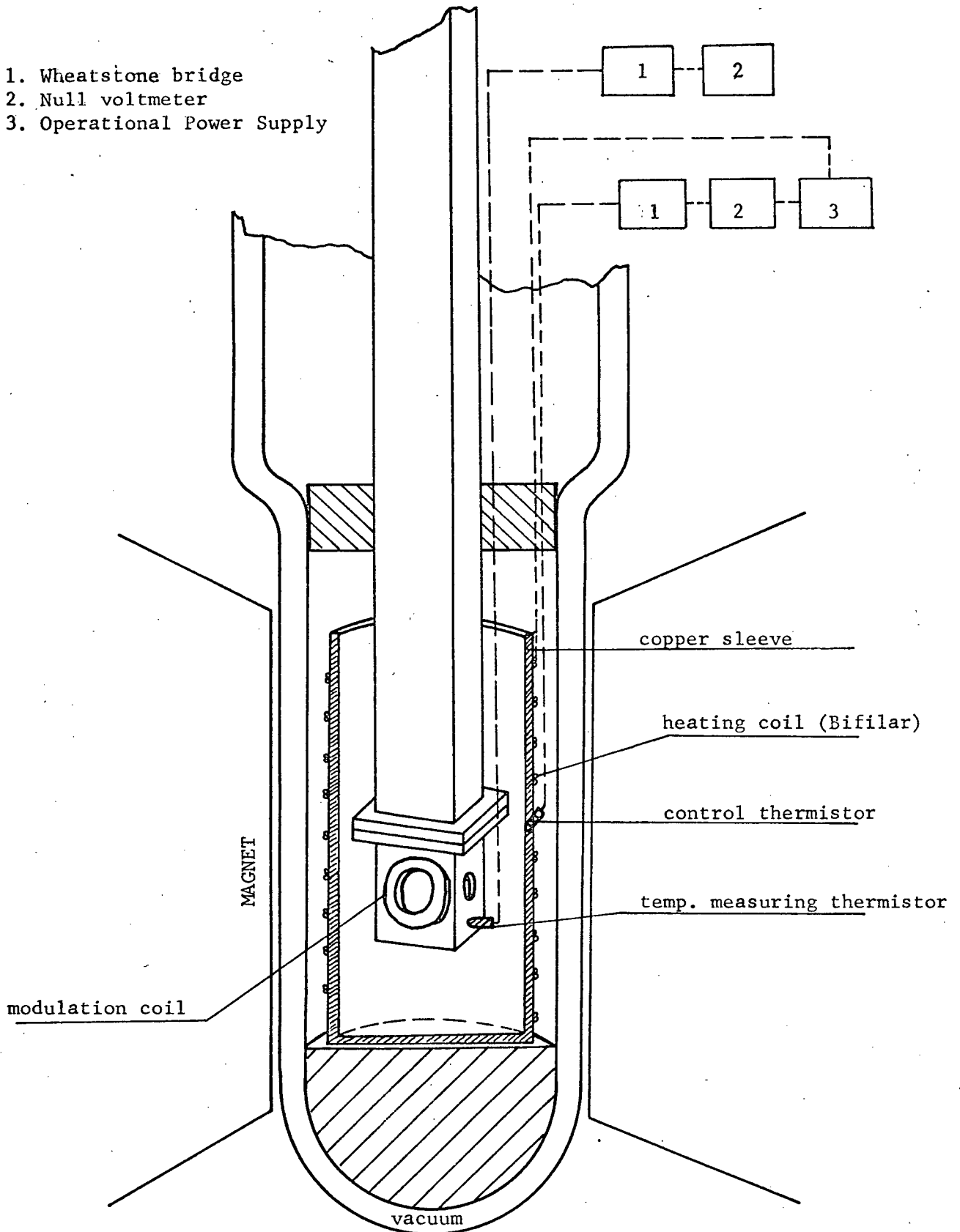


FIGURE 4.1 The heating system

CHAPTER 5

5.1 VISCOSITY OF NEMATIC LIQUID CRYSTALS

The main purpose of this work is a study of the EPR spectra of free radicals dissolved in nematic liquid crystals as a function of temperature. It is known that the ordering of the liquid crystal molecules causes large changes of the EPR hyperfine splitting of free radicals which have an anisotropic hyperfine interaction³. From the changes of the hyperfine splitting it is possible to obtain some information about the orientation and ordering of the liquid crystal molecules.

From the shapes of the absorption lines some conclusion about the dynamical properties of the liquid crystal solvent can be drawn. Studies of the line width of the absorption lines are very useful when correlation times of the molecular motion and interactions are studied. To estimate the correlation times of molecular motions using certain hydrodynamic models the dynamic viscosity of a liquid is needed. It is clear that the molecular interactions between solute-solvent molecules are not the same as solvent-solvent molecular interactions. Another problem might be the classical definition of the viscosity, which is not very appropriate on a micromolecular scale. Extensive studies of the EPR linewidths in isotropic solvents have shown that classically defined viscosities give relatively good agreement between theory and experiment⁴⁴. Although it is not likely that classical viscosity will give good agreement between theory and experiment in the nematic phase of a liquid crystal, a good agreement between theory and experiment may be expected in the isotropic phase of a liquid crystal. Therefore, the kinematic flow

viscosities of several nematic liquid crystals in the isotropic and nematic phases were measured. The temperature dependence of liquid crystal densities was not measured since liquid crystal densities are about $1\text{gr}/\text{cm}^3$ and hence the dynamic and kinematic viscosities are approximately equal.

The viscosity measurements were made with a Fenske 200-J781 capillary tube in a temperature controlled oil bath. The temperature was controlled with a contact thermometer and could be kept at the temperature $T \pm 0.1^\circ\text{C}$ when the viscosities of MBME and MBBA were measured, and at the temperature $T \pm 1^\circ\text{C}$ when the viscosity of HOAB was measured. Viscosities of the pure liquid crystals were measured. The paramagnetic impurities were added later. Measurements were always made from the isotropic phase to lower temperatures.

There is no simple relation which describes the temperature dependence of the viscosity of liquid over the entire temperature range. The Arrhenius relation

$$\log \eta = A + \frac{B}{kT} \quad (5.1)$$

accurately describes the viscosity of liquids of a simple molecular structure well above their melting points, but it does not hold for very viscous liquids. Therefore, it is not very surprising that it fails completely in the nematic phase of a liquid crystal.

The viscosity of the nematic liquid crystal is unique. Above the I-N phase transition temperature, liquid crystals behave as normal isotropic liquids. The I-N phase transition and its associated visual turbidness occur at a very steep viscosity decrease. The nematic

liquid crystal molecules are readily and highly oriented in the direction of the flow. Although, the studies of certain other properties of liquid crystals very close to the I-N transition show some pretransitional effects, no such effects have been observed in the viscosity measurements.

The flow viscosities of three liquid crystals in the isotropic and nematic phases have been measured and the results are shown in Figure 5.1. The error bars are shown for each curve separately.

The sharp changes in the viscosities at $T_R^* = 1.000$ are ascribed to changes in the molecular structure of liquid crystals.

5.2 THE I-N PHASE TRANSITION TEMPERATURE OF THE SYSTEM MBME + VACA

It has been pointed out that small concentrations of impurities may change the I-N phase transition temperature appreciably. To check how VACA changes the I-N phase transition temperature of the MBME a simple experiment was performed. A small quantity of the pure MBME and a small quantity of the mixture MBME + VACA (5.10^{-3} mole) were sealed into the evacuated glass ampules. Then both samples were heated at the temperature of 80°C for several days. The clearing temperature of the pure MBME and of the MBME - VACA mixture were recorded as a function of the time. The results are shown in Figure 5.2. In this figure it is apparent that the I-N phase transition temperature of the pure MBME was independent of prolonged heating, while the mixture I-N phase transition temperature was not. Therefore, care must be taken to assure that the correct phase transition temperature is known for the system under investigation.

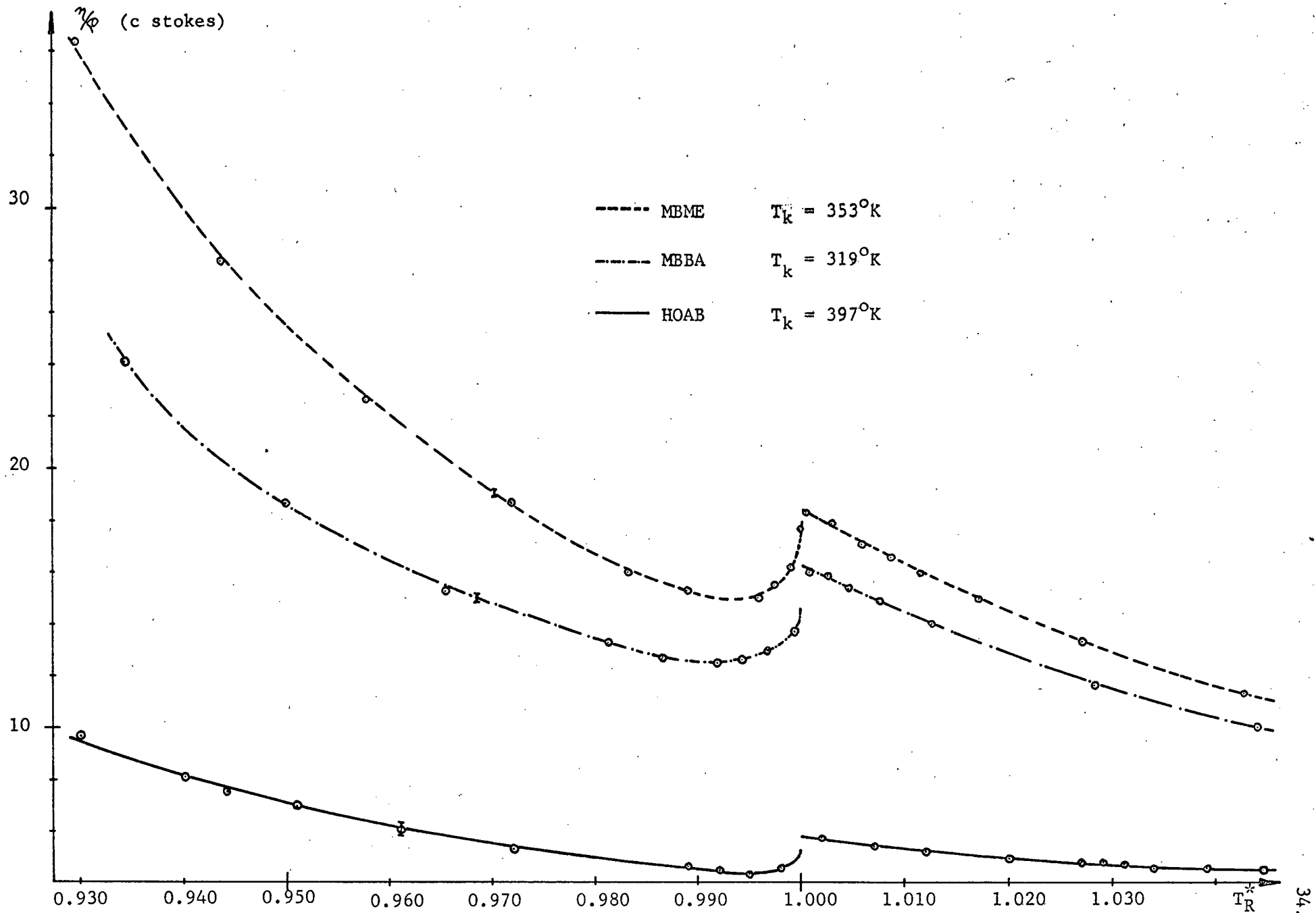


FIGURE 5.1 The viscosities and transitions temperatures of MBBA, MBME and HOAB.

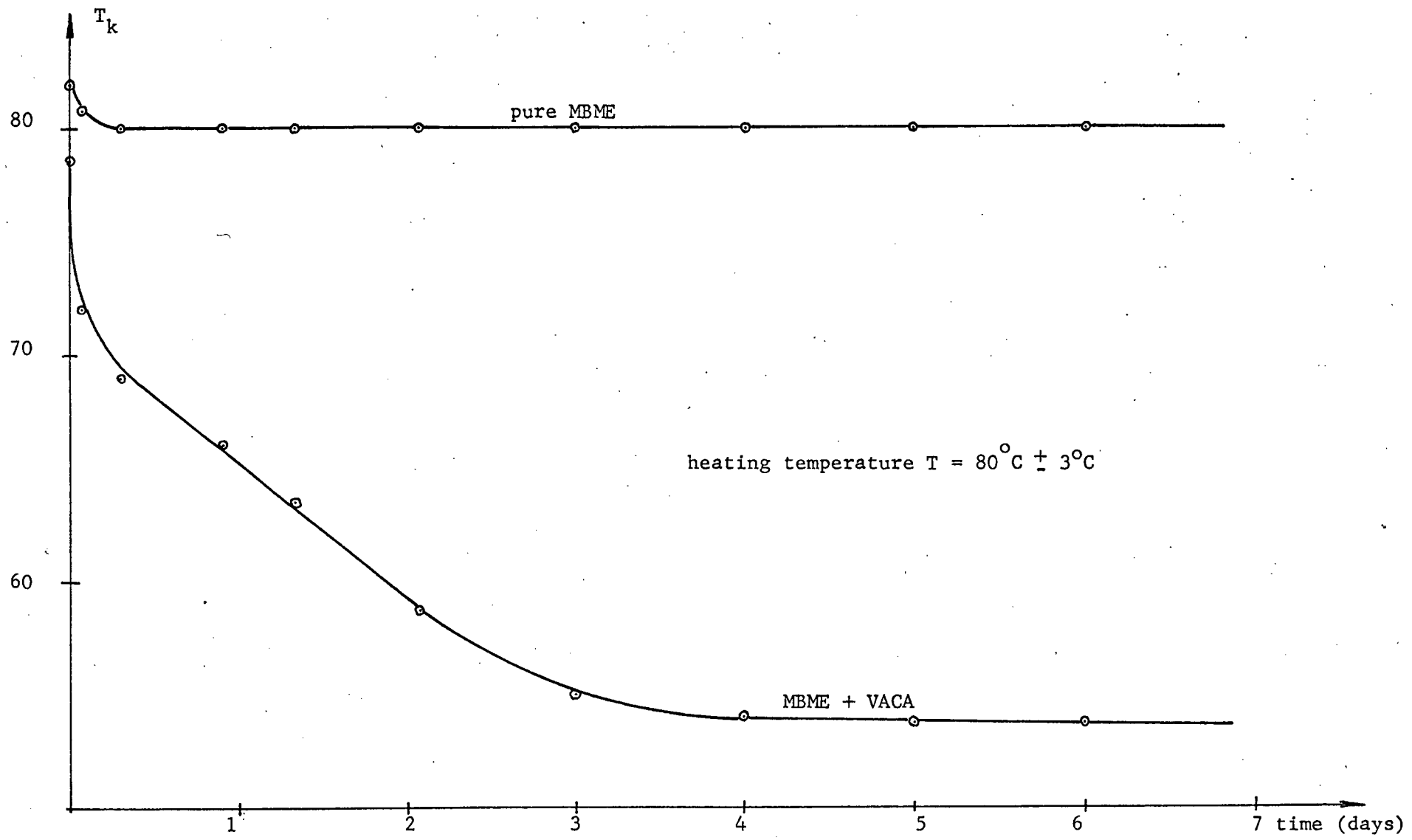


FIGURE 5.2 The I-N phase transition temperature of the system MBME + VACA as a function of the time.

CHAPTER 6

6.1 MAGNETIC RESONANCE IN LIQUID CRYSTALS

The first magnetic resonance experiments on liquid crystals were NMR experiments. Spence⁴⁵ and Weber³⁹ concluded that the difference in the NMR spectra between the isotropic and nematic phase results from the different ordering of the liquid crystal molecules in two phases.

It is possible to orient the molecules of an isotropic liquid with a help of a very strong d.c. electric field. The degree of the orientation by electric fields is very small. Saupe and Englert⁴⁶ first realized that the highly resolved spectrum of a simple solute dissolved in a liquid crystal should, in principle, be seen on the top of the broad unresolved spectrum of the liquid crystal. NMR spectra have been used to study¹ the geometry of solute molecules, the anisotropies of chemical shifts, the quadrupole coupling constant of deuterons, the mean orientation of the solute molecules in the anisotropic environment and also for the study of the intermolecular forces. The analyses of the NMR experiments give the order parameter of the liquid crystal or solute molecules. Results show that moderate concentrations of the solute molecules (up to 16%) do not, in general, change the order parameter of a pure liquid crystal³.

The EPR measurements are carried out by dissolving a small amount of a proper magnetic probe in the liquid crystal. The dissolved ions in a liquid solution exhibit a relatively stable short range order between the ion and the nearest surrounding solvent molecules. Complexes can form clusters which are similar to clusters found in solid crystals. There is, however, a fundamental difference in that the complex within

the liquid tumbles in a random way as it is pushed around by the molecular motions of the solvent liquid.

In normal liquids all directions are equivalent. If the solute moves in a random way and fast enough, the time dependent terms in the EPR spin Hamiltonian average to zero. However, if the solute motions are not too fast, it is possible to obtain some information about the molecular motions from the EPR spectrum.

The compounds which form liquid crystal phases are not, in general, paramagnetic. The EPR technique is, therefore, limited to solute studies where the solute molecule contains an unpaired spin.

One year after the Saupe-Englert discovery Carrington and Luckhurst⁴⁷ observed that EPR spectra from DPPH and tetracyanoethylene anion dissolved in the nematic phase of PAA, differ from the spectra of the same free radicals dissolved in the isotropic phase of the same compound. For the EPR studies a very low concentration of a free radical is needed (typically 10^{-4} - 10^{-3} mole). Such low impurity concentrations do not change the liquid crystal order parameter. Sometimes they change the phase transition temperature if the free radical slowly reacts with the studied liquid crystal.

It is obvious that solvent molecules affect motions and reorientation speeds of the solute molecules, although the factors determining the orientation of solutes in a nematic liquid crystal are not quantitatively understood. However, it is clear that in order for the solute to be oriented by a solvent, the solute-solvent intermolecular potential must be anisotropic. To observe the orientational effect of the solvent molecules on a solute molecule with an EPR experiment, the g-tensor and the hyperfine tensor have to be anisotropic and the molecule

has to have an appropriate geometrical shape. Free radicals with the anisotropic g- and hyperfine tensors, and with the spherical geometric shape do not show changes in the hyperfine splitting, when measured in the nematic and isotropic phase of a liquid crystal. Changes in the hyperfine splitting are very dependent on the solute size, shape and rigidity. Therefore, EPR measurements do not always show a true picture of a liquid crystal molecular organization. The comparing of our results with the results which were obtained by different experimental methods³⁹ show that SL103 dissolved in HOAB does not describe the real liquid crystal molecular ordering. The hyperfine splitting of SL103 dissolved in the HOAB does not change enough to give a degree of the partial alignment of the solute which would be in the agreement with the IR studies of the pure HOAB. We will see later that the EPR study using the SL103 gives $S_{\max} = 0.1 - 0.2$. However, IR measurements on the pure HOAB give $S_{\max} = 0.6 - 0.7$. On the other hand, VACA shows very well the degree of the liquid crystal order (Figure 7.9). Therefore, our conclusions will be drawn mainly from the system HOAB + VACA, although some results from the other systems will be shown, too.

6.2 THE ORDER PARAMETER OF FREE RADICALS DISSOLVED IN THE NEMATIC LIQUID CRYSTALS

The spin Hamiltonian for the VACA free radical is relatively simple, since the VACA molecule has only one unpaired electron and only one nuclear spin with which it interacts. The concentrations of free radicals used in this study were small enough that the electron-electron dipolar interactions could be neglected.

Using the irreducible tensor notation, the spin Hamiltonian for any paramagnetic probe, may be written as⁴⁸:

$$\mathcal{H} = \sum_{\mu|L,p} (-1)^p F_{\mu}^{(L,p)} T_{\mu}^{(L,-p)} \quad (6.1)$$

where μ denotes the type of an interaction, L is its rank, $F_{\mu}^{(L,p)}$ describes the strength of an interaction, p gives its component, and finally $T_{\mu}^{(L,-p)}$ is the p^{th} component of the appropriate spin operator. In equation (6.1) both $F_{\mu}^{(L,p)}$ and $T_{\mu}^{(L,-p)}$ are expressed in the same coordinate system. The functions $F_{\mu}^{(L,p)}$ are usually given in the molecular coordinate system, while the $T_{\mu}^{(L,-p)}$ are most conveniently described in the laboratory coordinate system. The irreducible spin operators in the equation (6.1) are written in the coordinate system which is fixed to the solute molecule. It is convenient to transform $T_{\mu}^{(L,-p)}$ to a laboratory coordinate system, since the external magnetic field suppresses a coordinate system and the spin states are usually quantized along magnetic field direction. Irreducible tensor operators transform under rotation with the help of the Wigner rotation matrices $\mathcal{D}_{q,-p}^{(L)}(\Omega)$. The transformed spin Hamiltonian is:

$$\mathcal{H} = \sum_{\mu|L,p,q} (-1)^p F_{\mu}^{(L,p)} \mathcal{D}_{q,-p}^{(L)} T_{\mu}^{(L,q)} \quad (6.2)$$

where

$$\mathcal{D}_{p,q}^{(L)}(\alpha\beta\gamma) = e^{-i p \alpha} d_{p,q}^{(L)}(\beta) e^{-i q \gamma}$$

α, β, γ are Euler angles⁴⁹. So, $F_{p,q}^{(L)}$ are constants of the given molecule and the time dependence of the spin Hamiltonian is given by the time dependence of the Wigner rotation matrices. To get the static spin Hamiltonian the ensemble or time average of the equation (6.2) has to be taken. Therefore,

$$\overline{\mathcal{H}} = \sum_{\mu; L, p, q} (-1)^p F_{\mu}^{(L, p)} \overline{\mathcal{D}_{q, -p}^{(L)}} T_{\mu}^{(L, q)} \quad (6.3)$$

As mentioned above for the VACA molecule the only important interactions are the coupling of the electron spin to the applied magnetic field and the nuclear spin of vanadium. These interactions can be of the zeroth or second rank tensors. Therefore, the spin Hamiltonian (6.3) is divided into two parts:

$$\overline{\mathcal{H}} = \overline{\mathcal{H}}^{(0)} + \overline{\mathcal{H}}^{(2)} \quad (6.4)$$

$\overline{H}^{(0)}$ is the isotropic part of the total spin Hamiltonian:

$$\overline{H}^{(0)} = \overline{H}^{(0)} = \sum_{\mu} F_{\mu}^{(0,0)} T_{\mu}^{(0,0)} \quad (6.5)$$

while $\overline{H}^{(2)}$ is the anisotropic part of the form:

$$\overline{H}^{(2)} = \sum_{\mu: p, q} (-1)^p F_{\mu}^{(2,p)} \overline{D}_{q, -p}^{(2)} T_{\mu}^{(2,q)} \quad (6.6)$$

In the isotropic liquid the molecules move in a random way. If the random motions are fast with respect to the Larmor frequency, then the time dependent terms in the expression (6.3) average to zero. This means that only the terms with $L = 0$ remains important and $\overline{H}^{(0)}$ has the form:

$$\overline{H}^{(0)} = \beta_e g H_0 S_z + a \vec{I} \cdot \vec{S} \quad (6.7)$$

where

$$\begin{aligned} g &= \frac{1}{3} (g_{xx} + g_{yy} + g_{zz}) \\ a &= \frac{1}{3} (A_{xx} + A_{yy} + A_{zz}) = F_{15}^{(0,0)} \end{aligned} \quad (6.8)$$

and β_e is the Bohr magneton.

It is assumed that the liquid crystal molecules affect the solute in such a way that their motion is no longer isotropic. A magnetic field stronger than two kilogauss, aligns the liquid crystal molecules parallel to the field. For the uniaxial nematic liquid crystals the alignment of molecules is axially symmetric about the direction of the magnetic field. It has been shown that the liquid crystal molecules align the solute molecules in a similar way to themselves⁵. Therefore, the required average value of the Wigner rotation matrix is

$$\overline{\mathfrak{D}_{q,-p}^{(l)}} = \int \mathfrak{D}_{q,-p}^{(l)}(\alpha\beta\gamma) f(\alpha\beta\gamma) d\Omega \quad (6.9)$$

The probability that a molecule has the orientation α, β, γ is given by $f(\alpha\beta\gamma)$. Assuming axial symmetry all values of α are equally probable, $f(\alpha\beta\gamma)$ is no longer dependent on α . The integral (6.9) vanishes if q is different from zero. The expression (6.4) reduces to the form:

$$\overline{H} = H^{(0)} + \sum_{\mu:p} (-1)^p F_{\mu}^{(2,p)} \overline{\mathfrak{D}_{0,-p}^{(2)}} T_{\mu}^{(2,0)} \quad (6.10)$$

The VACA free radical has all magnetic interactions axially symmetric. The components for $F_{IS}^{(2,p)}$ and $T_{IS}^{(2,p)}$ are⁵⁰:

$$T_{IS}^{(0,0)} = [I_z S_z + \frac{1}{2} (S^+ I^- + S^- I^+)] \quad (6.11)$$

$$F_{IS}^{(2,0)} = \left(\frac{1}{24}\right)^{\frac{1}{2}} (2A_{zz} - A_{xx} - A_{yy}) = -\left(\frac{3}{8}\right)^{\frac{1}{2}} b$$

$$T_{IS}^{(2,0)} = \left(\frac{8}{3}\right)^{\frac{1}{2}} \left[S_z I_z - \frac{1}{4} (S^+ I^- + S^- I^+) \right] \quad (6.11)$$

$$F_{IS}^{(2, \pm 1)} = 0 \quad F_{IS}^{(2, \pm 2)} = \frac{1}{4} (A_{xx} - A_{yy}) = \frac{1}{2} c$$

$$T_{IS}^{(2, \pm 1)} = \mp (S_z I^{\pm} + S^{\pm} I_z) \quad T_{IS}^{(2, \pm 2)} = S^{\pm} I^{\pm}$$

Because of the axial symmetry all $F_{\mu}^{(2,p)}$ terms are zero except the terms for which $p = 0$

$$\overline{\mathcal{H}} = \mathcal{H}^{(0)} + \sum_{\mu} F_{\mu}^{(2,0)} \overline{\mathcal{D}}_{0,0}^{(2)} T_{\mu}^{(2,0)} \quad (6.12)$$

Other coefficients of the irreducible tensors ($F_{\mu}^{(2,0)}$ and $T_{\mu}^{(2,0)}$) have been tabulated by Freed and Fraenkel⁵⁰. Their introduction into equation (6.12) gives:

$$\overline{\mathcal{H}} = \beta_e (g + \overline{\mathcal{D}}_{0,0}^{(2)} \Delta g) H_0 S_z + (a + \overline{\mathcal{D}}_{0,0}^{(2)} b) \vec{I} \cdot \vec{S} \quad (6.13)$$

where

$$\begin{aligned} \Delta g &= \frac{2}{3} (g_{\perp} - g_{\parallel}) & g_{xx} &= g_{yy} = g_{\perp} & g_{zz} &= g_{\parallel} \\ b &= \frac{2}{3} (A_{\parallel} - A_{\perp}) & A_{xx} &= A_{yy} = A_{\perp} & A_{zz} &= A_{\parallel} \end{aligned} \quad (6.14)$$

The liquid crystal spin Hamiltonian is therefore of the same form as the isotropic spin Hamiltonian. The only difference shows in the magnitude of the g -value and in the magnitude of the hyperfine constant. If we denote the liquid crystal g -value and the liquid crystal hyperfine splitting

constants by g' and a' , we have:

$$g' = g + \overline{D_{0,0}^{(2)}} \Delta g \quad (6.15)$$

$$a' = a + \overline{D_{0,0}^{(2)}} b$$

Fryburg and Gelerinter⁴³ defined the order parameter for the VACA dissolved in a nematic liquid crystal by

$$\mathcal{O} \equiv \frac{1}{2} \overline{(3 \cos^2 \beta - 1)} = \overline{D_{0,0}^{(2)}} \quad (6.16)$$

where now β is the angle between the director and the symmetry axis of the VACA molecule. The relationship between the order parameter for the liquid crystal molecules "S" and the order parameter for VACA free radical dissolved in a nematic liquid crystal, \mathcal{O} , is⁵:

$$S = -2\mathcal{O} \quad (6.17)$$

This is because of the definition of the Z-axis of the VACA molecule.

The EPR measurement of the hyperfine splitting in the nematic phase gives " a' " and hyperfine splitting measurement in the isotropic phase gives " a ". The constant " b " can be obtained by studying the VACA molecule in solid crystals or powders. From these data it is then possible to calculate the solute order parameter as a function of the temperature. Equations (6.15) then give:

$$\mathcal{O} = \mathcal{S}_{0,0}^{(2)} = \frac{a' - a}{b} = \frac{1}{2} \frac{a' - a}{a - A_1} \quad (6.18)$$

The order parameter for a nematic liquid crystal, S , theoretically has its value between 0 and 1. Therefore, the order parameter for the solute molecule VACA is between 0 and $\frac{1}{2}$. It has been found experimentally that the nematic liquid crystal order parameter has values between 0.3 and 0.9.

With a proper selection of the paramagnetic probe such as VACA the EPR experiment gives an order parameter which is consistent with the results of other experimental methods.

CHAPTER 7

7.1 HYPERFINE SPLITTING AND ORDER PARAMETER

The EPR spectrum of a paramagnetic molecule which possesses anisotropic magnetic interactions and rotates rapidly ($\omega > \omega_0$, where ω_0 is the Larmor frequency) in an isotropic medium, is relatively simple. For VACA, for example, it consists of eight slightly overlapping absorption lines. The lines are usually symmetric and the line shape is Lorentzian. The isotropic hyperfine splitting between such lines is given by

$$a = \frac{1}{3}(A_{xx} + A_{yy} + A_{zz})$$

where A_{ii} are components of the hyperfine splitting parallel to the i -th molecular axis. If the hyperfine interactions are axially symmetric

$$a = \frac{1}{3}(A_{\parallel} + 2A_{\perp})$$

where A_{\parallel} and A_{\perp} are given by equations (6.14). The positions of the absorption lines are given (to first order) by:

$$H = \frac{2}{g} H_0 - a m_x$$

where H_0 is the field corresponding to $g = 2$ at the spectrometer frequency. A typical spectrum of the VACA dissolved in a low viscosity oil is shown in Figure 7.1a.

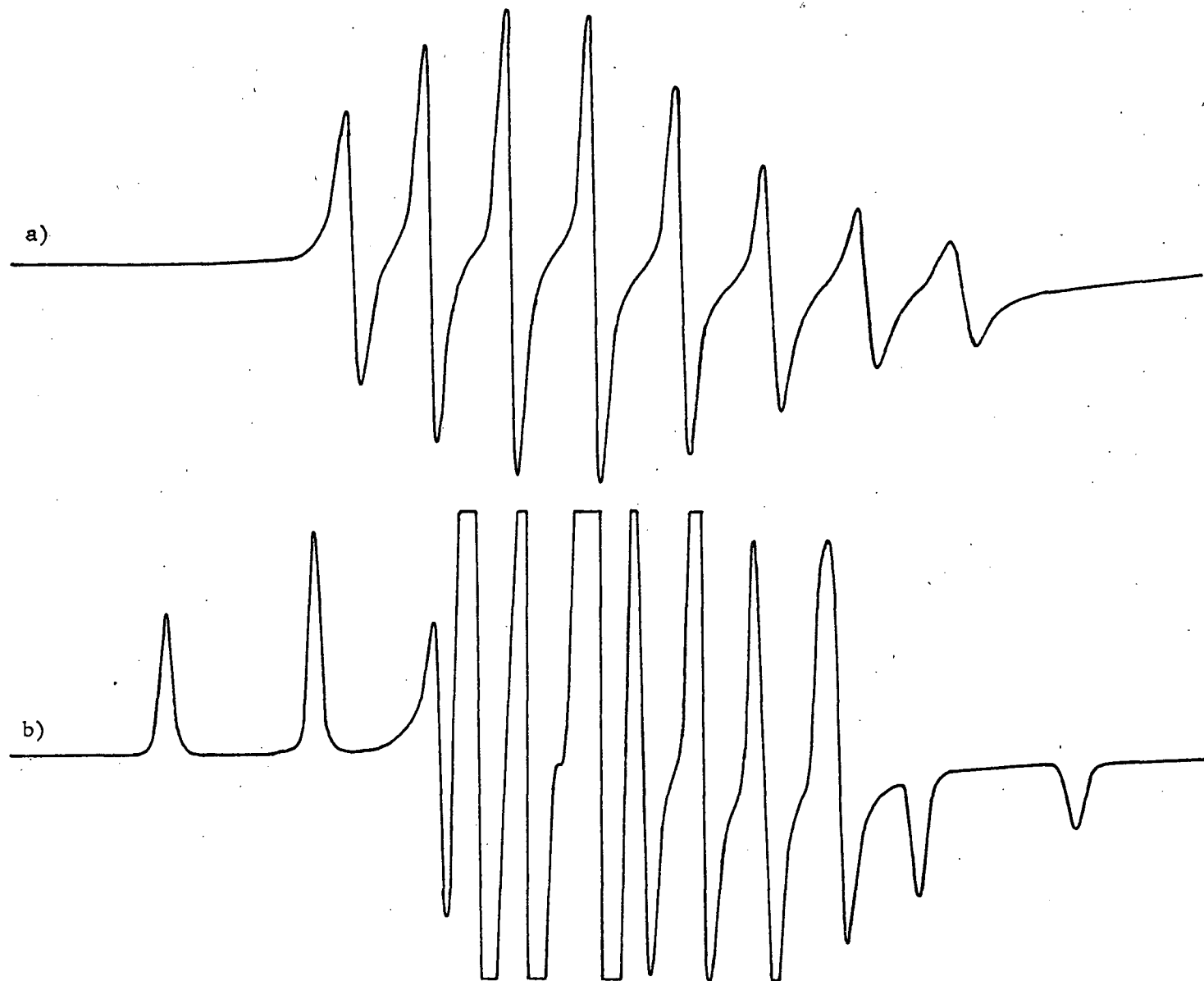


FIGURE 7.1 The first derivative of the absorption lines of
a) VACA in a low viscosity liquid (Octofoil at $T = 115^{\circ}\text{C}$)
b) VACA in a high viscosity liquid (Octofoil at $T = 25^{\circ}\text{C}$)

Another (extreme) situation can be met if a solvent is so viscous that it seriously hinders the rotation of the paramagnetic molecule ($\omega \ll \omega_0$). From such a system a "powder type" spectrum results. The shape of such absorption lines become complicated and careful studies of such lines give information about the anisotropies of the g- and hyper-fine splitting tensors. From "powder studies" the data in table I (page 25) were determined.

Positions of the absorption lines for the paramagnetic molecule with the axially symmetric magnetic interactions become dependent on the angle β between Z-axis of paramagnetic molecules and the external magnetic field. They are given by⁴³

$$H = \frac{2H_0}{g_{\parallel}^2 \cos^2 \beta + g_{\perp}^2 \sin^2 \beta} - A m_I - \frac{A_{\perp}^2}{4H_0} \frac{A^2 + A_{\parallel}^2}{A^2} [I(I+1) - m_I^2] \quad (7.1)$$

where

$$A^2 = \frac{A_{\parallel}^2 g_{\parallel}^2 \cos^2 \beta + A_{\perp}^2 g_{\perp}^2 \sin^2 \beta}{g_{\parallel}^2 \cos^2 \beta + g_{\perp}^2 \sin^2 \beta}$$

An absorption line of such a system is composed of many Lorentzian lines. When there is no preferred orientation of the paramagnetic molecules the number of molecules with a certain orientation is proportional to $\sin \beta d\beta$. This can be combined with the equation (7.1) to obtain the absorption line shape. In viscous nematic liquid crystals a proper distribution function for the molecular orientation has to be used⁵¹. For isotropic liquids such calculations have been published⁵².

The resultant line shape for the paramagnetic molecule with axially symmetric interactions is shown in Figure 7.2.

Between these two extreme viscosity ranges there is a viscosity range where molecular motions are neither fast enough to give a simple well averaged spectrum, nor slow enough to give powder spectrum. The EPR spectrum of such a system can be very complicated.

Two of the liquid crystals which we studied (the MBME and MBBA), have viscosities in this intermediate range such that the VACA motions start to be seriously hindered at a temperature $\sim 10^{\circ}\text{C}$ above the I-N phase transition.

Also in normal liquid as the viscosity increases a powder spectrum starts to appear so that by merely decreasing the temperature it is possible to study the development of the powder spectrum. The intensities of the parallel components of the hyperfine splitting increase until their final intensity is reached and further increasing of the liquid viscosity does not affect them any more. The first derivative of an absorption VACA spectrum in a very viscous isotropic liquid (vacuum oil) is shown in Figure 7.1b.

It is well known that a magnetic field of the proper strength orients the low viscosity liquid crystal molecules^{7,51}, when a liquid crystal is in its nematic phase. Previous investigations have shown that the VACA molecule are affected by the liquid crystal molecules in such a way that the probability that the VACA symmetry axis points in the direction perpendicular to the external magnetic field is larger than the probability that the VACA symmetry axis point parallel to the magnetic field. This is evidenced by the fact that even when the molecules are

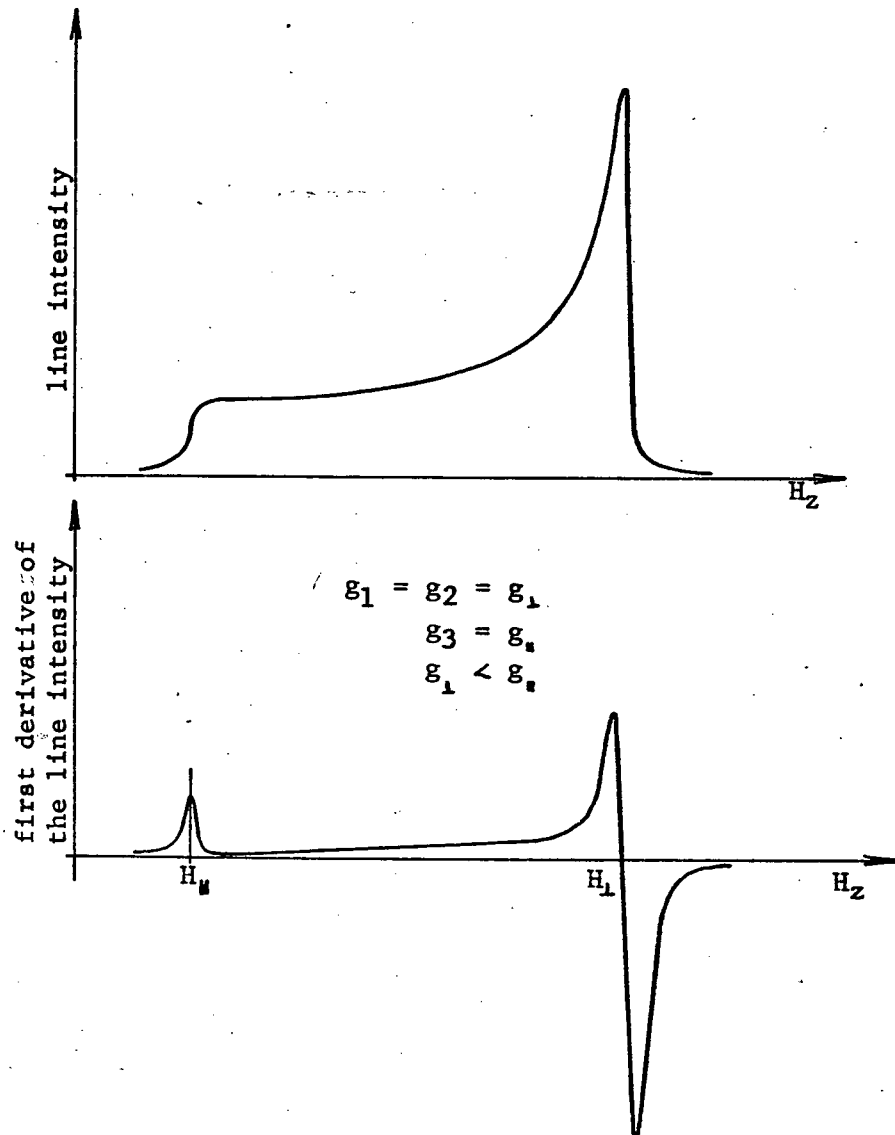


FIGURE 7.2 The "powder" absorption line of a paramagnetic probe with axial symmetry

completely frozen the parallel component of hyperfine lines intensities of the VACA molecules in a nematic liquid crystal are smaller than the intensities of the same components in an isotropic liquid of the same viscosity. This is shown in Figure 7.3a,b. If the ordering of a nematic liquid crystal were perfect ($S = 1$), the EPR spectrum would give only the perpendicular component of the hyperfine splitting, A_{\perp} .

Many liquid crystals upon which previous measurements have been made, have viscosities in the range where molecular rotation is hindered to such an extent that the EPR spectra are intermediate between motionally narrowed and powder spectra. This means that the measured hyperfine splitting, and hence the deduced order parameter, are not given by equations (6.15) and (6.18). The present combined EPR and viscosity measurements were the first to demonstrate this fact⁹. In reality it means that the hyperfine splitting cannot be determined by merely measuring the experimental distance between the lines of the spectrum. Qualitatively this explains why the order parameter deduced by Chen and Luckhurst for several nematic liquid crystals does not fall on the theoretically calculated curve of the order parameter versus reduced temperature.

In Figure 7.4 the hyperfine splitting of the VACA dissolved in the MBME is shown. Curve I gives the hyperfine splitting as measured between the first and eighth (first derivative) peaks. Thus measured hyperfine splitting starts to decrease already far in the isotropic phase of the MBME. This is mainly caused by the increasing viscosity of the liquid crystal. The same effect is observed in an isotropic liquid such as pump oil. Upon cooling the oil becomes very viscous and the apparent hyperfine splitting changes monotonically.

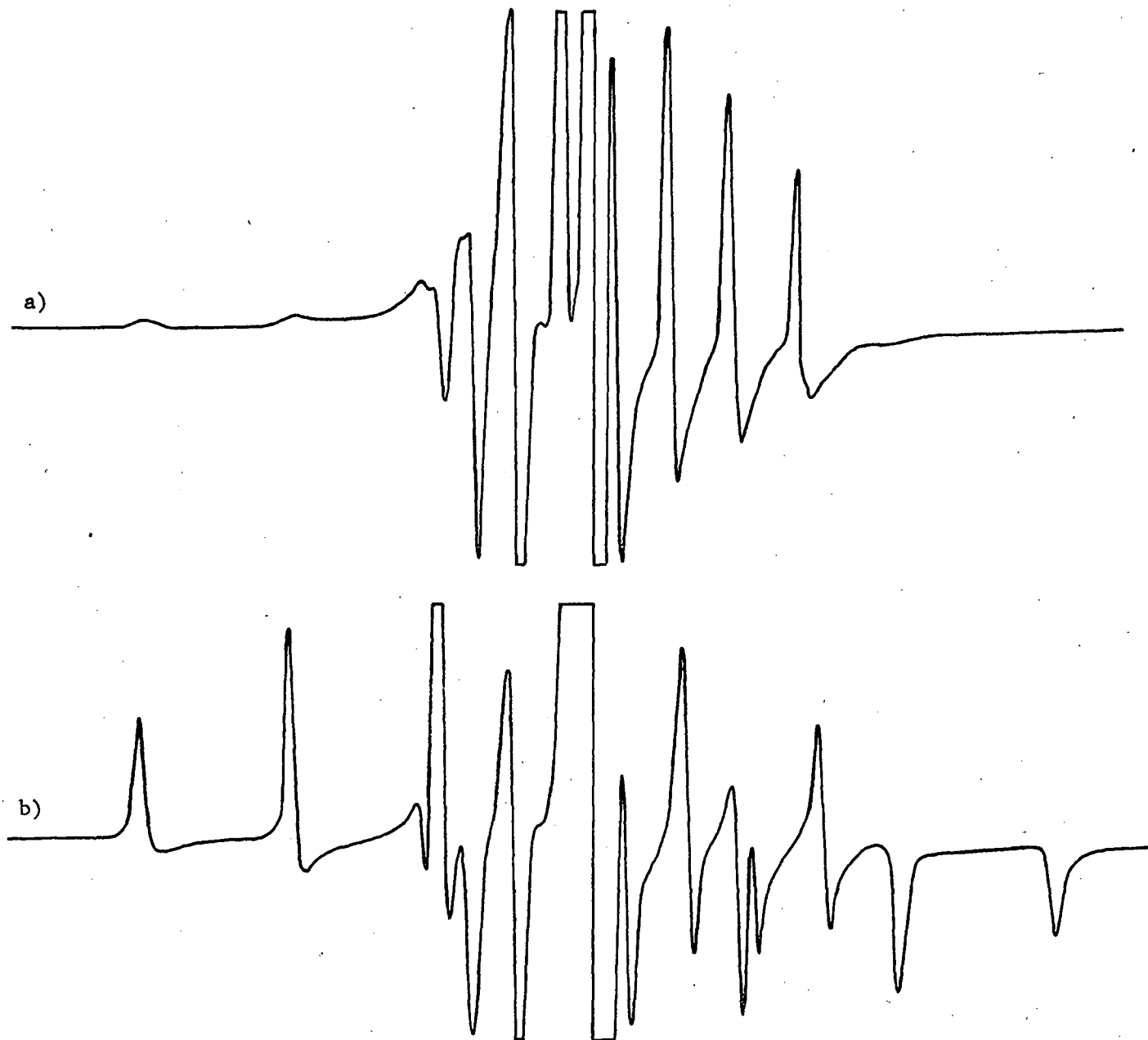


FIGURE 7.3 The first derivative of the absorption lines of
 a) VACA in MBME ($H \parallel \vec{n}$, $T = -50^\circ\text{C}$)
 b) VACA in MBME ($H \perp \vec{n}$, $T = -50^\circ\text{C}$)

The effect of viscosity on the hyperfine splitting of the VACA dissolved in the MBME is minimized if one measures the distance between the hyperfine lines of $m_I = -\frac{1}{2}$ and $m_I = -3/2$. This hyperfine splitting is shown by curve II in Figure 7.4. The order parameter calculated from such measurements can serve as an estimate only.

In Figure 7.3a one sees that the MBME molecules hinder the motions of the VACA molecules to such an extent that the absorption lines become very broad and asymmetric even at temperatures above the I-N phase transition. To eliminate the overlapping of the absorption lines the same measurements were repeated with SL103. It has been mentioned that the EPR spectrum of SL103 consists of only three well resolved lines arising from the hyperfine interaction of the electron spin with the nitrogen nuclear spin $I = 1$.

From the line widths of the hyperfine lines it is possible to conclude that the SL103 molecules dissolved in the MBME move much faster than those of VACA dissolved in the same solvent. The motional average is, therefore, much better in the system MBME + SL103 than it is in the system MBME + VACA. In this system (MBME + SL103) the parallel components of the hyperfine splitting were not observed even at temperatures well below room temperature. At a temperature of 50°C the lines overlap only slightly and the positions where the resonances occur are not affected.

Changes of the SL103 hyperfine splitting upon decreasing the temperature through the I-N phase transition are small. The temperature dependence of the hyperfine splitting of the system MBME + SL103 is shown in Figure 7.5. The order parameter as calculated from the hyperfine splitting in Figure 7.5 is much smaller than the order parameter as calculated from the measurements with the VACA molecule. It has been

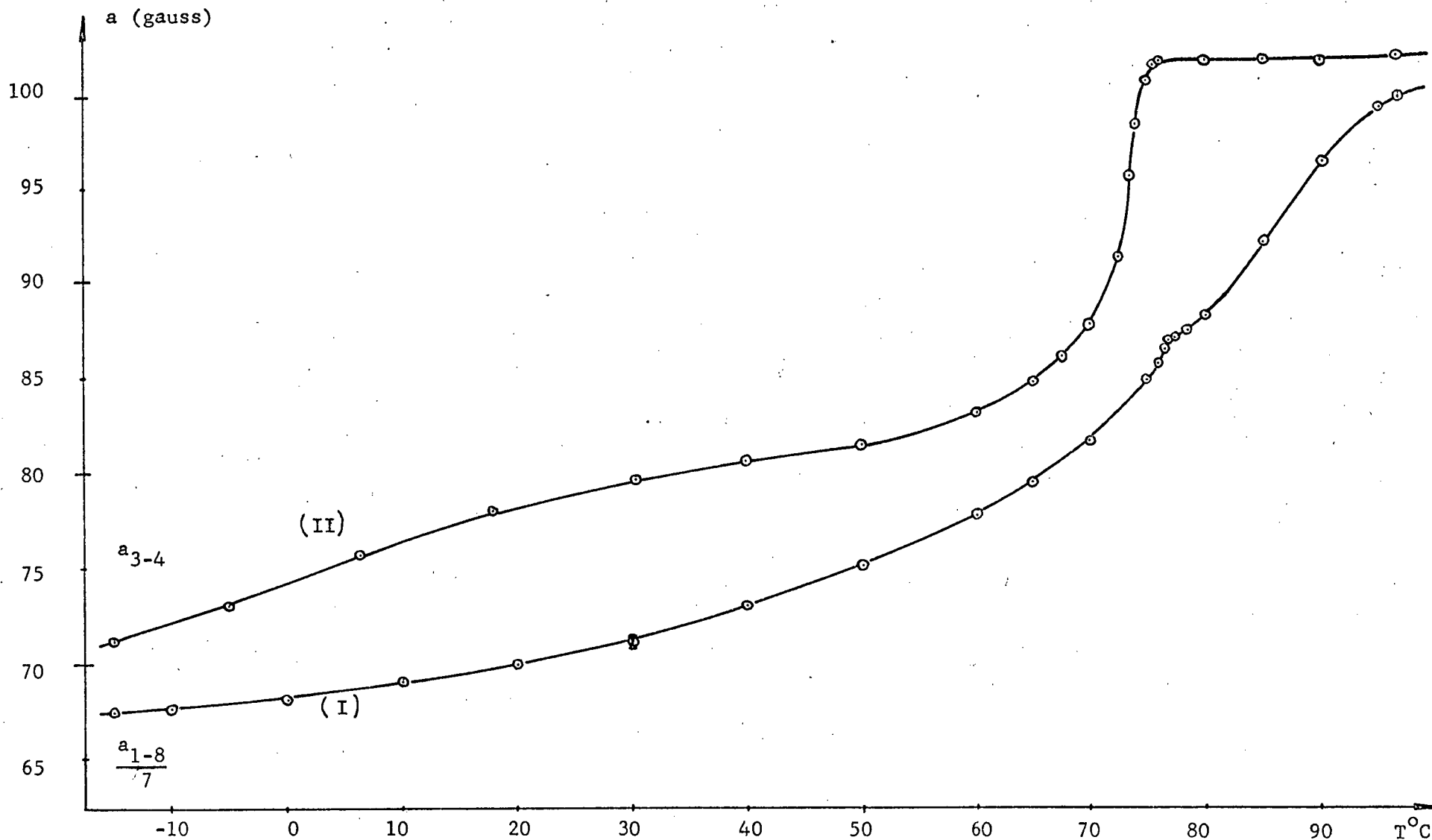


FIGURE 7.4 The hyperfine splitting of the VACA dissolved in the MBME as a function of the temperature.

Curve I (II) gives the hyperfine splitting as measured between the hyperfine lines of $m_I = -7/2$

and $m_I = 7/2$ ($m_I = -3/2$ and $m_I = -1/2$).

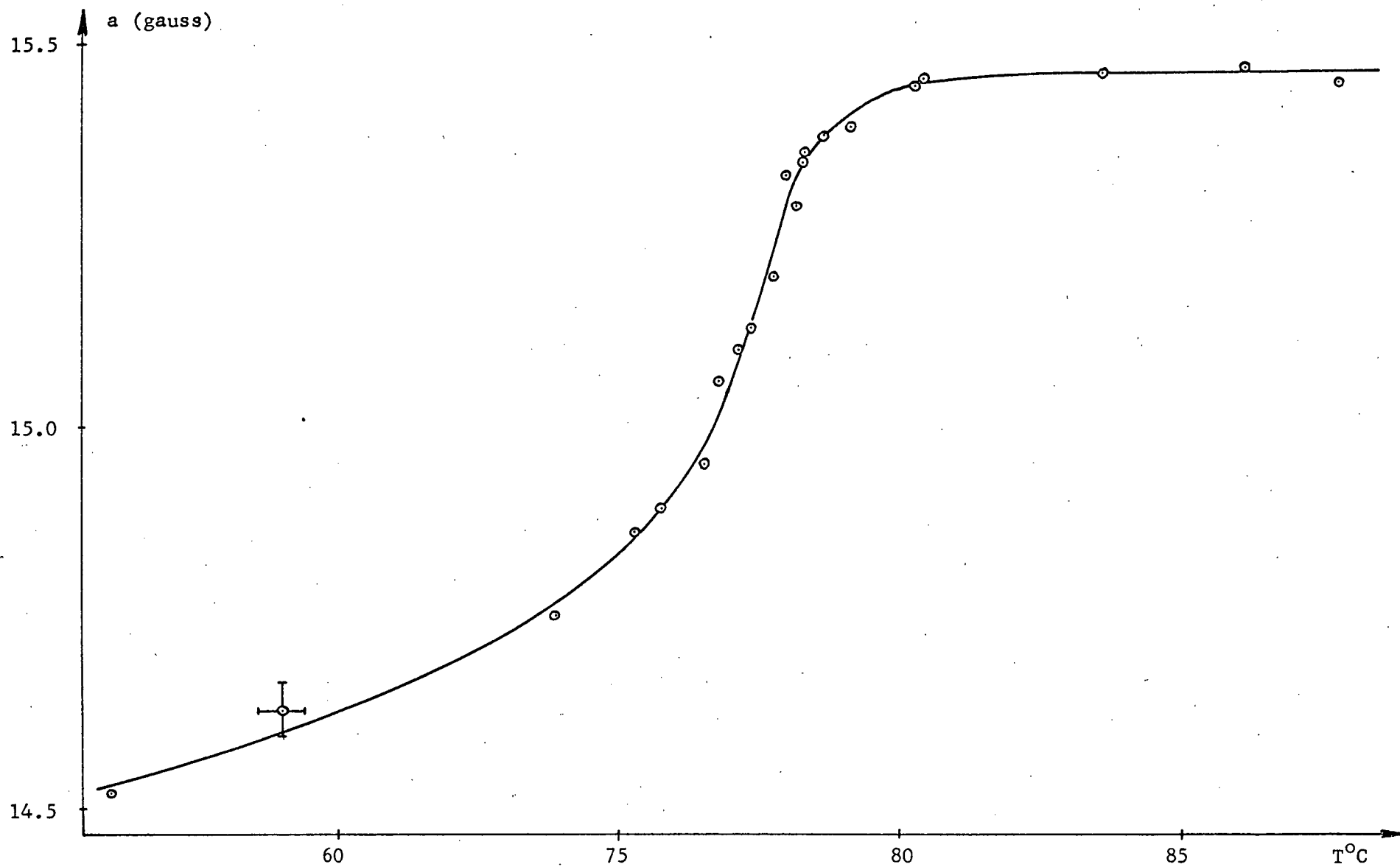


FIGURE 7.5 The hyperfine splitting of the SL103 dissolved in MBME as a function of the temperature.

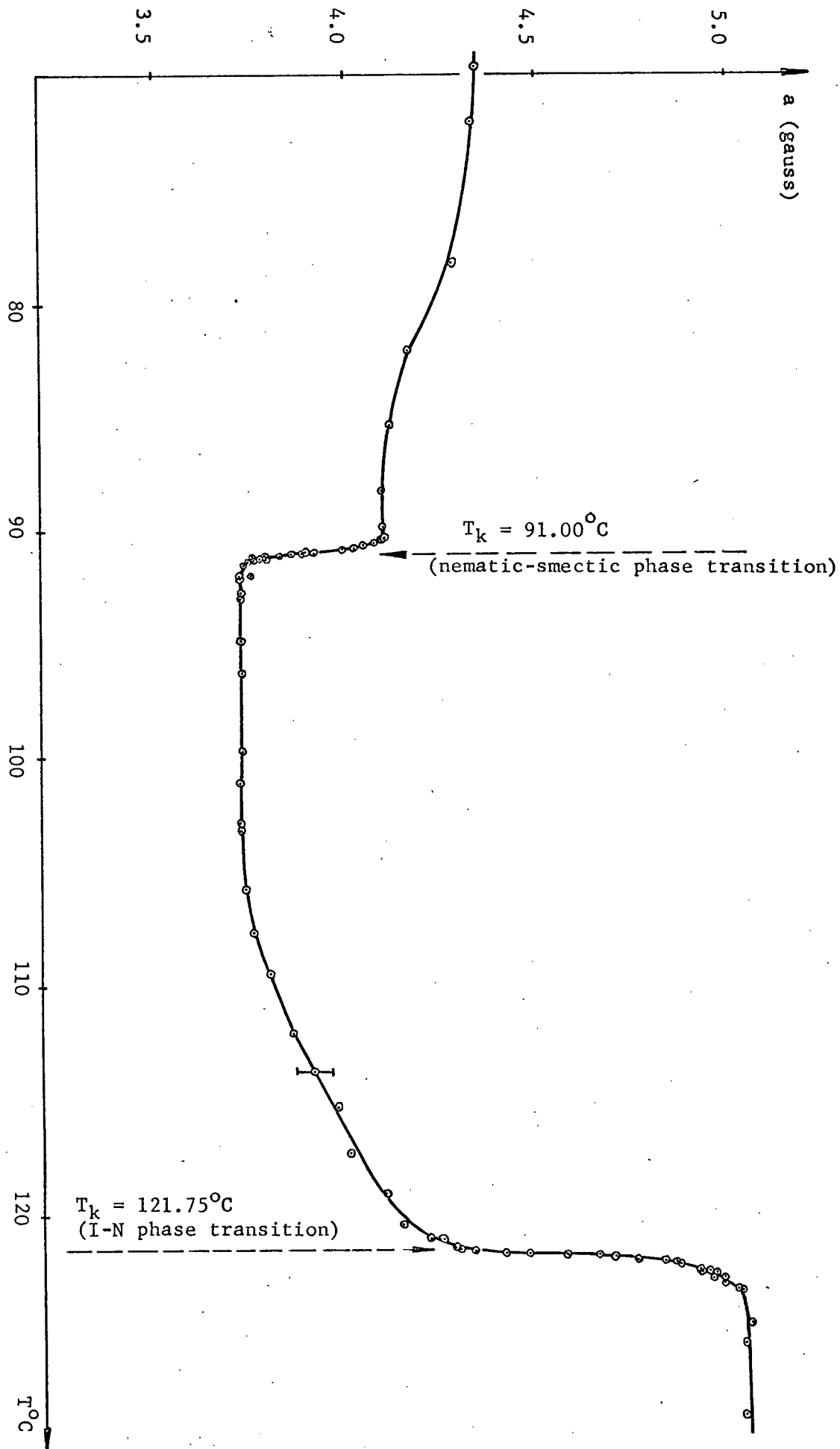
shown ^{3,43} that the vanadyl molecules dissolved in nematic liquid crystals reflect the molecular alignment of solvent molecules very well. Since the order parameter obtained from the EPR spectrum of the SL103 molecule was considerably smaller than the order parameter of the VACA we conclude that the SL103 molecule is not a very good paramagnetic probe to study the order parameter of the nematic liquid crystals which are discussed in this work.

To eliminate the overlapping of the absorption lines of VACA as much as possible, a liquid crystal with a lower viscosity than that of the MBME was chosen. Since VACA and SL103 molecules are very stable when dissolved in the 4,4-di-n-heptoxyazoxybenzene (HOAB) and their EPR spectrum is relatively simple the liquid crystal HOAB was chosen for the main studies of this thesis.

Our study of the system MBME + SL103 has shown that SL103 does not describe the ordering of the MBME molecules satisfactory. However, since we are interested in the changes of the hyperfine splitting of the system liquid crystal-paramagnetic molecule at temperatures near to the phase transition, we measured the hyperfine splitting of the system HOAB + SL103.

A typical concentration of the SL103 dissolved in HOAB was 10^{-4} mole and therefore we may ignore the electron dipolar interactions. This concentration does not alter the I-N phase transition temperature of the HOAB. The experiments were performed by using a well controlled heating system (Figure 4.1). It has been pointed out that the HOAB possesses two liquid crystal phases, namely, a nematic phase and a smectic phase. The hyperfine splitting in both phases as a function of the temperature is shown in Figure 7.6.

FIGURE 7.6 Hyperfine splitting of the SL103 dissolved in the HOAB as a function of the temperature.



The EPR spectrum of the SL103 in HOAB consists of three hyperfine lines even when the HOAB is in the smectic phase which has high viscosity. (If the system HOAB + SL103 in its smectic phase is rotated 45° with respect to the external magnetic field, an unusual splitting of the high field hyperfine line appears, however this effect will not be discussed in this thesis). No parallel components of the hyperfine splitting were observed, however the absorption lines broadened in the smectic phase.

In Figure 7.7 the hyperfine splitting of the system HOAB + SL103 in the nematic phase is shown as a function of the reduced temperature (a reduced temperature is defined by $T_R^* = \frac{T}{T_k}$, T_k is the clearing temperature). The I-N phase transition temperature in this experiment was taken to be $T_k = 121.75^\circ\text{C}$. At this temperature the change of the hyperfine splitting is the steepest. One sees that the hyperfine splitting begins to change $1 - 2^\circ\text{C}$ above the phase transition temperature. The absolute temperature was accurate to $\pm 1^\circ\text{C}$, but relative temperature measurements were better than $\pm 0.01^\circ\text{C}$. Figure 7.7 also shows that in the nematic phase below 105°C the hyperfine splitting remains constant. The order parameter for SL103 dissolved in HOAB is shown in Figure 7.9, curve II.

Since the VACA molecules describe the alignment of nematic liquid crystals better, the system HOAB + VACA was mainly studied. The solutions investigated contained less than 10^{-3} mole of the paramagnetic probe and hence avoided electron spin-electron spin dipolar interactions. The addition of VACA to HOAB (concentration 10^{-3} mole) lowers the I-N transition temperature by about 2°C .

Since the viscosity of HOAB is about three times lower than the viscosity of the MBME the absorption lines of the system HOAB + VACA

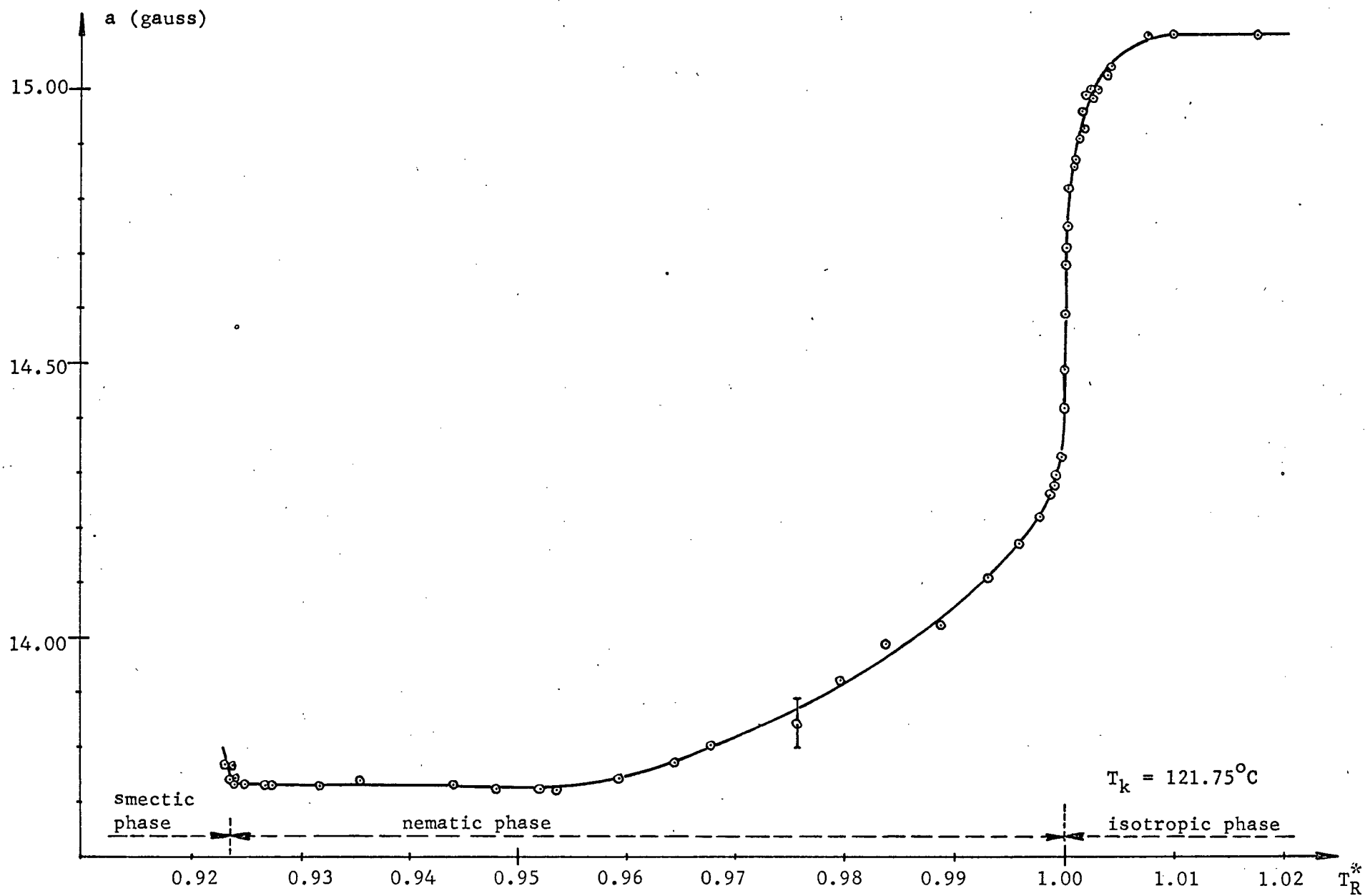


FIGURE 7.7 The hyperfine splitting of the SL103 dissolved in the nematic phase of the HOAB as a function of the reduced temperature.

are, in general, narrower than the hyperfine lines of the system MBME + VACA. The overlapping of these lines is therefore smaller than in the previous case. From the lineshapes of the spectrum it is possible to conclude that the motional average is good and the positions of absorption lines are represented by equation (7.2) and are not seriously affected by overlapping.

Measurements were performed in the isotropic and nematic phases. The isotropic splitting of VACA is larger than the isotropic hyperfine splitting of SL103. The hyperfine splitting changes considerably when lowering the temperature from the isotropic to the nematic phase (Figure 7.8). The order parameter which was obtained from these measurements is shown in Figure 7.9, curve I. In this figure one sees that the order parameter of the system HOAB + VACA is much larger than the order parameter of the system HOAB + SL103 and it is consistent with NMR³⁹ and optical measurements. This indicates that the VACA molecule reflects the molecular organization of the HOAB fairly well. This is in some way surprising since the maximal linear dimension of the VACA as studied by the X-rays⁵³ turns out to be about four times smaller than a similar dimension of the HOAB. Although the VACA molecules are much smaller than the liquid crystal molecules, the liquid crystal molecules in the nematic range affect motions of the VACA in such a way that the hyperfine splitting changes $\sim 20\%$. From the magnitude of the hyperfine splitting it is possible to conclude that the symmetry axis of the hyperfine interactions of the VACA dissolved in the HOAB nematic phase is aligned perpendicular to the external magnetic field and this means that the long VACA molecular axes are (partially) aligned parallel to the liquid crystal long molecular axes. The I-N phase transition temperature is taken as that temperature where the

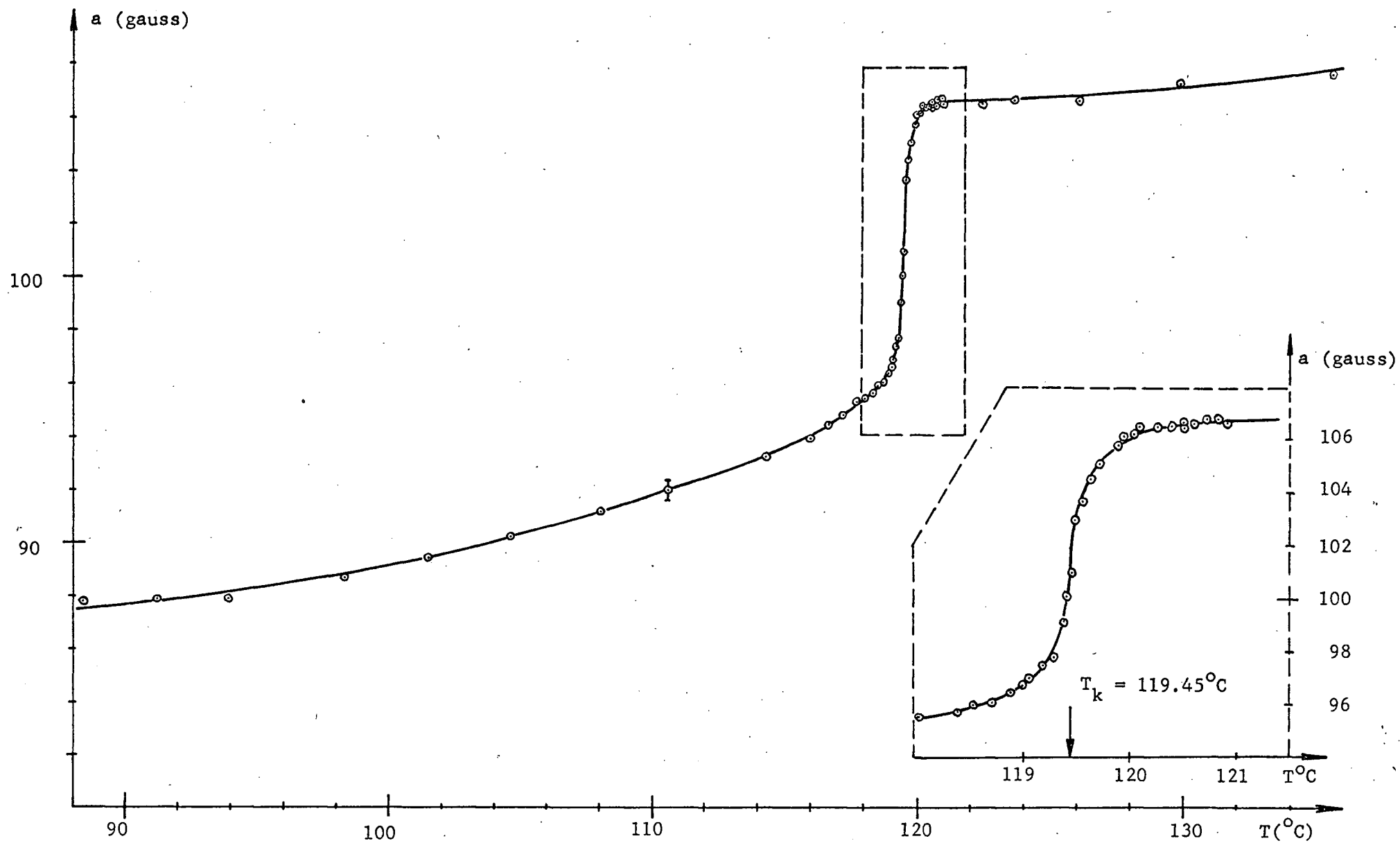


FIGURE 7.8 The hyperfine splitting of the VACA dissolved in HOAB as a function of the temperature.

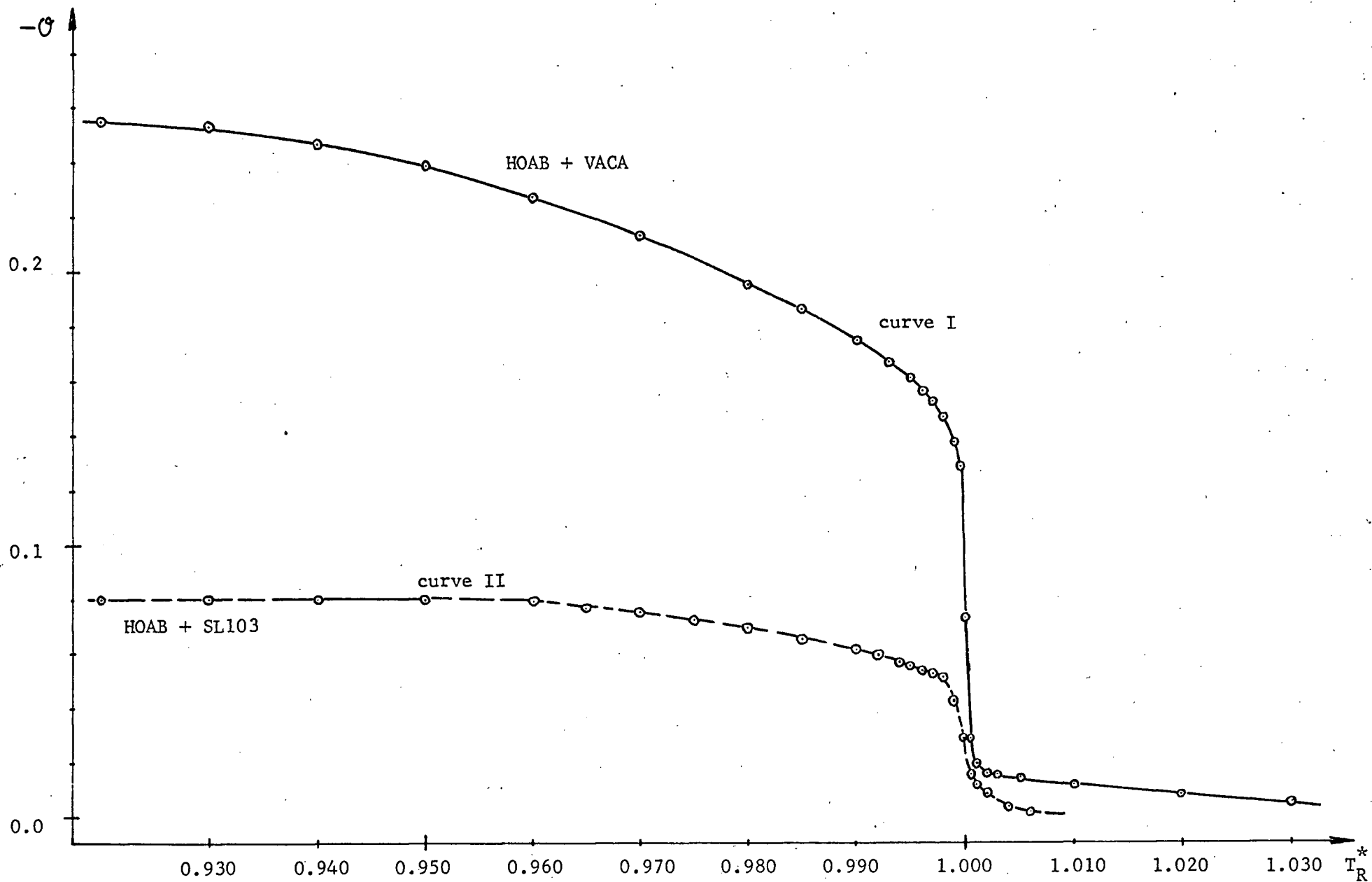


FIGURE 7.9 The order parameter of the SL103 and VACA dissolved in the HOAB nematic phase as a function of the reduced temperature.

slope of the hyperfine splitting versus temperature is the steepest,

$$T_k = 119.45^\circ\text{C}.$$

A computer program (written by J. Maruani) was used to fit the theoretical and experimental spectra. The program is written for Lorentzian or Gaussian lineshapes, axially symmetric magnetic interactions and isotropic solutions. In the isotropic phase far above the I-N phase transition temperature, the experimental and theoretical calculated spectra using Lorentzian lineshape agreed very well. On approaching the I-N phase transition temperature from above the agreement worsened. Just above the I-N phase transition temperature better agreement was obtained by using Gaussian lineshapes rather than the Lorentzian. Since the program is written for isotropic motions of the probe molecules, the positions of the absorption lines at the middle of a spectrum could not be fitted, because the liquid crystal molecular ordering is not taken into account. From the equation (6.13) the line positions for paramagnetic molecule with axial symmetry in the nematic phase is given by:

$$H_{m_I} = \frac{2}{g} H_0 - (a + \overline{D_{0,0}^{(2)}} b) m_I - \frac{1}{2H_0} (a - \frac{1}{2} \overline{D_{0,0}^{(2)}} b)^2 [I(I+1) - m_I^2] \quad (7.2)$$

In the isotropic phase $\overline{D_{0,0}^{(2)}}$ vanishes and equation (7.2) reduces to the form:

$$H_{m_I} = \frac{2}{g} H_0 - a m_I - \frac{a^2}{2H_0} [I(I+1) - m_I^2]$$

From these two equations it becomes obvious why the agreement with the experimental spectra was not better. From the directions of the shifts of the hyperfine lines in the middle of the spectrum in the nematic phase with respect to the position of the hyperfine splitting lines in the isotropic phase of the same liquid crystal, it is possible to conclude that the liquid crystal molecular ordering begins before the actual phase transition temperature is reached.

At this point it might be proper to comment on the order parameter at the I-N phase transition temperature. Maier-Saupe's theory gives ^{1,24} a discontinuous order parameter, S , at the phase transition temperature and the minimum value of S should be 0.32. Since short range order is always present in liquid, theory assumes that in the isotropic liquid the molecules form small spherical groups of nearest neighbours. This assumption led to the derivation of a reduced equation of state for the order parameter which should be universally valid. The theory suggests that at the transition temperature (T_k) all nematic liquid crystals should have approximately the same magnitude for the order parameter, $S = 0.44$.

No conclusion can be drawn from our measurements on the system HOAB + SL103. The order parameter of the VACA molecules dissolved in the HOAB is shown in Figure 7.9, curve I. From this curve it is clear that the order parameter determined from the EPR spectra does not confirm Maier-Saupe's conclusions about S at T_k . It has been pointed out that VACA dissolved in the HOAB gives the actual order parameter of the pure HOAB. In Figure 7.9 one sees that the order parameter of the VACA at T_k does not exceed the value 0.25. If the present results are accurate two possibilities have to be considered. The first is that Maier-Saupe's

theory is not valid at the I-N phase transition temperature. The second possibility is that VACA does not show what actually happens very close to the T_k . Data from the present measurements only are not adequate to confirm either of these possibilities. More experiments are clearly needed.

It has been mentioned that small groups of molecules are always present in isotropic liquids. The electrical birefringence in the isotropic phase of the PAA has been explained³⁰ by such groups. Stinson and Litster^{31a,b} studied the magnetically induced birefringence in the isotropic phase of the MBBA. Their results show that it is possible to align a nematic liquid crystal molecules in the isotropic phase with a magnetic field. Thus hyperfine splitting of VACA in the isotropic phase of the HOAB could be explained by assuming that the correlation length for the orientational motion of the small groups increases as the system approaches the phase transition temperature from above. Interaction between the external magnetic field and the total magnetic moment of the correlated groups increases and thus enhances the alignment of these groups by a magnetic field. The present results indicate that very close to T_k the external magnetic field interactions start to overcome thermal fluctuations. The thermal fluctuations of the groups decrease. Careful studies of the hyperfine splitting at T_k with different magnetic fields could supply more information about the molecular alignment in the isotropic phases of liquid crystals. For EPR measurements this would require spectrometers with several different frequencies.

As a conclusion to this chapter it is worthwhile to mention an interesting feature of the measurements. The results show that the nematic liquid crystals orient two different paramagnetic probes to a different extent, but the ratio of the order parameters for both probes

is the same in all nematic liquid crystal. For example, if the nematic liquid crystal (A) orients paramagnetic probe (1) so that its order parameter is " \mathcal{O}_1 " and paramagnetic probe (2), so that its order parameter is " \mathcal{O}_2 ", then the ratio $\mathcal{O}_1/\mathcal{O}_2$ is roughly the same in all nematic liquid crystals. Measurements of this type could be very useful in studies of different probes in well known nematics.

CHAPTER 8

ELECTRON SPIN RELAXATION IN LIQUID CRYSTALS8.1 INTRODUCTION

In this chapter we will describe our measurements and results done on the system HOAB + SL103 and HOAB + VACA.

A free radical molecule dissolved in a liquid serves as a small probe which helps one to "see" the solvent molecular organization and motions. The EPR line shapes and linewidths are dependent on solvent motions. Therefore the EPR spectrum of a free radical may contain a wealth of information about solvent molecular motions. Clearly, the dissolved solute molecules affect the solvent molecular motions. To what extent solvent properties are changed is not understood completely. However, it has been observed experimentally^{5,55} that some of the solvent properties do not change upon the addition of diamagnetic or paramagnetic materials if the concentrations of these are small enough. Many experimental studies are done with commercially produced materials. The purity of such materials is not extremely high (usually, $\sim 1\%$). The addition of $\sim 0.01\%$ of a free radical does not change the total concentration of impurities appreciably.

Many extensive studies and reviews of the electron paramagnetic relaxation of free radicals dissolved in the isotropic liquids have been reported^{44,50,56}. It appears that theories are quite successful when the molecular motions are very rapid or very slow, but several unsolved problems remain in the intermediate region.

In EPR studies two external magnetic fields are needed. The static external magnetic field H_0 determines the direction of quantization of spins. An oscillating microwave field $2H_1 \cos \omega t$ which is perpendicular to H_0 causes transitions between the electron spin states.

In addition to being influenced by these two fields, the electron spin of the probe molecule is coupled to local magnetic fields associated with the orientation of the probe molecule itself, and of the neighbouring solvent molecules. These local fields are time-dependent since the positions and orientations of the solvent molecules (and hence, also those of the probe) are constantly changing.

It is possible to obtain information about the solvents from the shapes and widths of the EPR absorption lines, providing that one can identify the sources of the local fields which broaden the lines. Roughly speaking, two types of line broadening mechanisms must be considered. Fluctuations in the local field at a frequency corresponding to the difference in energy between two spin states, can induce transitions between them. This gives rise to the broadening of the energy levels of these states because of their finite lifetime.

The second mechanism is associated with the existence of a distribution of local magnetic fields in the substance. In solids broad lines are observed, the widths of the lines being a measure of the spread of local fields. In liquids, the motion of the molecules "averages" the local fields experienced by any given spin so that the EPR line becomes narrower than in the solids ("motional narrowing"). Usually, the effects of molecular motion are treated using the theory of stochastic processes⁵⁷ The results of such a theory by Glarum and Marshall⁵ which is appropriate for the interpretation of our experiments will be discussed below.

The molecular motions in nematic liquid crystals are not isotropic. One expects, however, that the isotropic phase of a liquid crystal will not differ very much from a normal, low viscosity, isotropic liquid. However, below the I-N phase transition temperature certain re-orientational motions become hindered and this causes characteristic changes of the relaxation time.

In recent years several publications have appeared^{5,6,58} where the line shapes and linewidths of the free radicals dissolved in nematic crystals were discussed. Glarum and Marshall⁵ investigated the influence of a nematic liquid crystal solvent on the paramagnetic relaxation of the vanadyl complexes. They showed that for a high degree of molecular orientational order and in viscous solvents the secular processes are quenched so that pseudosecular processes* become most important. Their calculations show the linewidths (ΔH) can be well described by the equation

$$\Delta H(m_z) = A + Bm_z + Cm_z^2 \quad (8.1)$$

where A, B, and C are parameters which depend on temperature and whose form will be given later, " m_z " is the V^{51} nuclear spin magnetic quantum number. The relation between the transverse relaxation time, T_2 , and the linewidth determined by the separation of the

* The words "secular" and "pseudosecular" are used by Glarum and Marshall to denote contributions to the line widths from spectral densities of the local fields near zero frequency and the frequency corresponding to the hyperfine splitting, respectively.

maximum and minimum of the first derivation of an absorption line is given by

$$\Delta H = \frac{2\hbar}{\sqrt{3}g\beta} \frac{1}{T_2} \quad (8.2)$$

for Lorentzian lines.

Equation (8.1) is a truncated form of the equation given in reference⁵⁹ which describes the linewidths of free radicals dissolved in isotropic liquids. The theory gives two more terms which are proportional to " m_1^3 " and " m_1^4 ". Experiments with isotropic liquids have shown⁴² that these two terms are very small and do not affect the experimental line widths appreciably. Therefore we ignore them in our discussion.

Glarum and Marshall⁵ described the liquid crystal molecular motions by a single correlation time. It is generally believed that because of the highly anisotropic nature of the liquid crystal solvent the assumption of a single correlation time, which is independent of the instantaneous molecular orientation, is a rather crude approximation.

Nordio and Busolin⁵⁸, Rigatti and Segre⁶ studied the electron spin relaxation processes for paramagnetic molecules dissolved in nematic liquid crystals by solving the diffusion equation for the molecules oriented by an anisotropic intermolecular potential. They found that the components of the anisotropic interactions relax with several characteristic times. If the liquid crystal ordering were perfect, according to this theory all the characteristic times would go to zero, which would cause any contribution to the linewidth from the secular and pseudo-secular terms to vanish. Both, Glarum⁵ and Nordio^{6,58} discuss only g-tensor and hyperfine interactions and their final equations for the line-

widths are identical to equation (8.1). The only difference is the description of the molecular motions by a single correlation time (Glarum & Marshall) and by several correlation times (Nordio).

8.2 DYNAMIC SPIN HAMILTONIAN

In section 6.2 the static spin Hamiltonian for an axially symmetric free radical in a nematic liquid crystal was given by equation (6.10). That spin Hamiltonian gives only the magnetic fields of the absorption peaks. To study the dynamic properties of a liquid crystal one has to use the dynamic spin Hamiltonian, $\mathcal{H}'(t)$, which is given by

$$\mathcal{H}'(t) = \mathcal{H}(t) - \overline{\mathcal{H}} = \sum_{p,\mu} F_{\mu}^{(2,p)} \left[\mathcal{D}_{0,p}^{(2)}(t) - \overline{\mathcal{D}_{0,0}^{(2)}} \right] T_{\mu}^{(2,0)} \quad (8.3)$$

Glarum and Marshall⁵ treated this Hamiltonian following the procedure of Abragam⁵⁷ for an isotropic liquid. They obtained the expression (8.1).

The coefficients A, B, and C have the forms

$$\begin{aligned} A &= \frac{2\hbar}{\sqrt{3}g\beta_e} \frac{1}{4} (\Delta\gamma H_0)^2 [4J_0(\omega_0) + 3J_1(\omega_0)] + \\ &\quad + \frac{2\hbar}{\sqrt{3}g\beta_e} \frac{1}{4} b^2 I(I+1) [3J_1(a) + J_0(\omega_0) + 3J_2(\omega_0)] \\ B &= \frac{2\hbar}{\sqrt{3}g\beta_e} \frac{1}{2} (b\Delta\gamma H_0) [4J_0(\omega_0) + 3J_1(\omega_0)] \\ C &= \frac{2\hbar}{\sqrt{3}g\beta_e} \frac{1}{4} b^2 [8J_0(\omega_0) + 6J_1(\omega_0) - 3J_1(a) - J_0(\omega_0) - 3J_2(\omega_0)] \end{aligned} \quad (8.4)$$

The spectral densities $J_0(\omega)$, $J_1(\omega)$ and $J_2(\omega)$ in the equations (8.4) are given by

$$\begin{aligned}
 J_0(\omega) &= \frac{9}{4} \langle \cos^4 \beta - \langle \cos^2 \beta \rangle^2 \rangle j(\omega) \\
 J_1(\omega) &= \frac{3}{2} \langle \cos^2 \beta - \cos^4 \beta \rangle j(\omega) \\
 J_2(\omega) &= \frac{3}{8} \langle (1 - \cos^2 \beta)^2 \rangle j(\omega)
 \end{aligned}
 \tag{8.5}$$

These equations are the same as those of Glarum & Marshall. Glarum & Marshall used a single correlation time, τ_c , to describe the molecular motions in liquid crystals. They assumed that the correlation function decays exponentially. Therefore, their derivation gives

$$j(\omega) = \frac{2\tau_c}{1 + \omega^2\tau_c^2} \tag{8.6}$$

The correlation time, τ_c , is a rough measure of the time over which some orientational correlation exists for an assembly of molecules. In the Glarum & Marshall theory the correlation time of the paramagnetic solute molecule is assumed to be the same as for the solvent molecules and given by the Debye equation⁵⁷.

$$\tau_c = \frac{4\pi}{3k} \frac{\eta}{T} r^3 \tag{8.7}$$

Where "r" is the hydrodynamic radius of the solute molecule, and η is the viscosity* of the fluid. Equation (8.7) is derived for the case when the solute molecules are much larger than the solvent molecules, and when all motions of the solute molecules are isotropic.

In an isotropic liquid $J_0(\omega)$, $J_1(\omega)$ and $J_2(\omega)$ simplify to

$$J_0(\omega) = J_1(\omega) = J_2(\omega) = \frac{1}{5} j(\omega) \tag{8.8}$$

*Perhaps, more appropriate viscosity coefficient needed here would be

Studies of the VACA dissolved in the isotropic liquids have shown^{42,60} that the assumption of a single correlation time and of an exponential correlation function, gives fairly good agreement between theory and experiment. From the experimental linewidths in the isotropic phase of a liquid crystal one can calculate the coefficients A, B, and C in equation (8.1). Then with the help of equation (8.4), (8.7), and (8.8) it is possible to calculate the hydrodynamic radius of the dissolved free radical. A brief inspection shows that in equations (8.4) $J(\omega_0)$ may be ignored and $J(a)$ may be approximated by $J(0)$ for the isotropic phases. When these two approximations are valid the coefficients A, B, and C for the isotropic case reduce to the forms

$$\begin{aligned}
 A_{\text{iso}} &= \frac{2\hbar}{\sqrt{3} B \beta_e} \frac{1}{4} (\Delta\gamma H_0)^2 \frac{4}{5} j(0) + \frac{2\hbar}{\sqrt{3} B \beta_e} \frac{1}{4} b^2 I(I+1) \frac{3}{5} j(0) \\
 B_{\text{iso}} &= \frac{2\hbar}{\sqrt{3} B \beta_e} \frac{1}{2} (b \Delta\gamma H_0) \frac{4}{5} j(0) \\
 C_{\text{iso}} &= \frac{2\hbar}{\sqrt{3} B \beta_e} \frac{1}{4} b^2 j(0)
 \end{aligned}
 \tag{8.9}$$

The molecular motions in the nematic phase are not described adequately by a single correlation time^{2,61} and therefore equations (8.6) and (8.7) are not valid. One may also ask: What is the time development of the correlation function when molecular motions are highly anisotropic? At the present time this is not understood. We will use Glarum & Marshall expressions for A, B, and C without attempting to use a specific form for the time development of the correlation function. We assume that the absolute values of the spectral densities do not change very much in going from the isotropic phase to the nematic phase of a liquid crystal. Therefore, the spectral densities $J(\omega_0)$ will be ignored again. The equations

(8.4) give

$$\begin{aligned}
 A_{\text{NEM}} &= \frac{2\hbar}{\sqrt{3}g\beta_e} \frac{1}{4} (\Delta\gamma H_0)^2 4J_0(0) + \frac{2\hbar}{\sqrt{3}g\beta_e} \frac{1}{4} b^2 I(I+1) \cdot 3J_1(a) \\
 B_{\text{NEM}} &= \frac{2\hbar}{\sqrt{3}g\beta_e} \frac{1}{4} (b \Delta\gamma H_0) 4J_0(0) \\
 C_{\text{NEM}} &= \frac{2\hbar}{\sqrt{3}g\beta_e} \frac{1}{4} b^2 [8J_0(0) - 3J_1(a)]
 \end{aligned}
 \tag{8.10}$$

where

$$\begin{aligned}
 J_0(0) &= \frac{9}{4} \langle \cos^4\beta - \langle \cos^2\beta \rangle^2 \rangle j(0) \\
 J_1(a) &= \frac{3}{2} \langle \cos^2\beta - \cos^4\beta \rangle j(a)
 \end{aligned}
 \tag{8.11}$$

and "a" is the hyperfine splitting constant at a certain temperature.

From equation (8.11) and experimental data one can calculate $j(0)$ and $j(a)$. To do this the averages $\langle \cos^2\beta \rangle$ and $\langle \cos^4\beta \rangle$ are required. One can relate $\langle \cos^2\beta \rangle$ to the order parameter, \mathcal{O} , which can be determined from the hyperfine splitting (see Chapter 6). The average $\langle \cos^4\beta \rangle$ has to be calculated, since no simple measurement gives it. To calculate this average a distribution function for the molecular orientations is needed. It has been suggested⁶² that the main contribution to the intermolecular potential in liquid crystals comes from dispersion forces and therefore the orientational distribution function for liquid crystal molecules has the form

$$P(\beta) = \text{const.} e^{-\lambda^2 \sin^2\beta}
 \tag{8.12}$$

where λ is a constant.

Recent studies have shown⁶³ that $P(\beta)$ does not describe the molecular distribution well, but that it does give an adequate first approximation to the order parameter. Attempts have been made^{63,64} to get a better expression for the intermolecular potential energy in liquid crystals. However, these new results do not change our interpretation very much, and therefore we will use the distribution function given by equation (8.12) in our calculation.

To calculate $\langle \cos^4 \beta \rangle$ the constant λ in (8.12) must be determined. The order parameter of a solute with the axially symmetric magnetic interactions, \mathcal{O} , can be calculated from the hyperfine splitting

$$\mathcal{O} = -\frac{1}{2} S = \frac{a' - a}{a - A_1}$$

From the definition of the liquid crystal order parameter one has

$$\langle \cos^2 \beta \rangle = \frac{1}{3} (2S + 1) = \frac{\int \cos^2 \beta P(\beta) d\Omega}{\int P(\beta) d\Omega} = \frac{1}{2\lambda^2} \left(\frac{\lambda e^{\lambda^2}}{P(\lambda)} - 1 \right) \quad (8.13)$$

where

$$P(\lambda) = \int_0^\lambda e^{t^2} dt$$

From (8.13) it follows that

$$S(\lambda) = \frac{3}{4\lambda^2} \left(\frac{\lambda e^{\lambda^2}}{P(\lambda)} - 1 \right) \div \frac{1}{2} \quad (8.14)$$

In Figure 8.1 $S = S(\lambda)$ is plotted. Using this curve and the dependence of the order parameter on temperature, the coefficient $\lambda = \lambda(T)$, and hence $\langle \cos^4 \beta \rangle$, can be obtained.

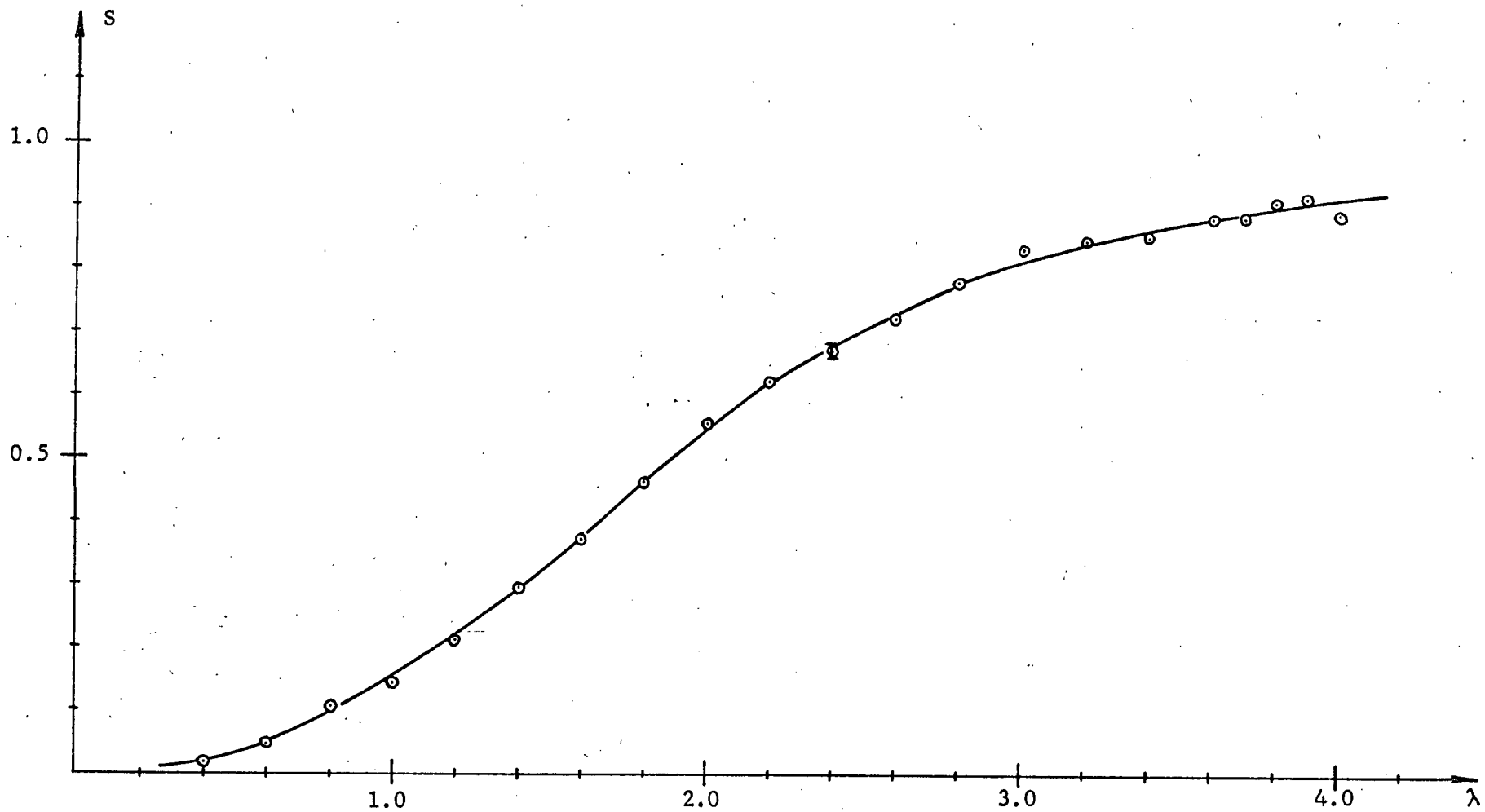


FIGURE 8.1 The order parameter as a function of the parameter λ

Before concluding this chapter a comment on the validity of the Glarum & Marshall relaxation theory might be appropriate. At temperatures more than 5°C above the I-N phase transition the experimental absorption lineshapes of the system HOAB + VACA are Lorentzian. At the temperatures very close to the nematic-smectic phase transition ($\sim 2^\circ\text{C}$) the lineshapes are again Lorentzian. The lineshapes are definitely not Lorentzian very close to the I-N phase transition. Therefore it appears that the condition

$$|\chi'(t)\tau_c|^2 \ll 1 \quad (8.15)$$

which has to be fulfilled in order that the theory be valid, holds in the nematic phase and in the isotropic phase of the HOAB, but does not hold very close to the nematic-isotropic phase transition temperature.

CHAPTER 9

EXPERIMENTAL RESULTS9.1 THE WIDTHS OF THE ABSORPTION LINES OF THE SYSTEM HOAB + SL103

We have shown in Chapter 6 that the SL103 does not describe the order parameter of the HOAB satisfactorily. Therefore, no detailed comparison between theory and experiment will be given for this system. However, these results are interesting because they show that the linewidths are quite sensitive to the I-N phase transition even for the system where the order parameter is small. The results of our experiments are shown in Figure 9.1. The spectrum of SL103 consists of three lines and their linewidths were measured in the isotropic, nematic and smectic phases. From the plotted data we can see that the low magnetic field line ($m_I = 1$) is the narrowest one. The low magnetic field line and the middle line ($m_I = 0$) do not change very much at the phase transitions. The changes in linewidths for these two lines are smaller than the estimated experimental error. At temperatures below 95°C the low field line become even narrower. A similar effect has been observed⁶⁵ for the system p-azoxyanisole + 4,4'-terphenylene nitroxide biradical. This narrowing of the low magnetic field line was explained by the spin-rotational interaction.

The temperature change of the high field absorption line ($m_I = -1$) are quite different from those of the other two lines. Though the width of this line does not change very much over the whole nematic range it has a sharp maximum at the I-N transition. Studies of the spectra of spin labels such as SL103 in isotropic liquids invariably show increasing

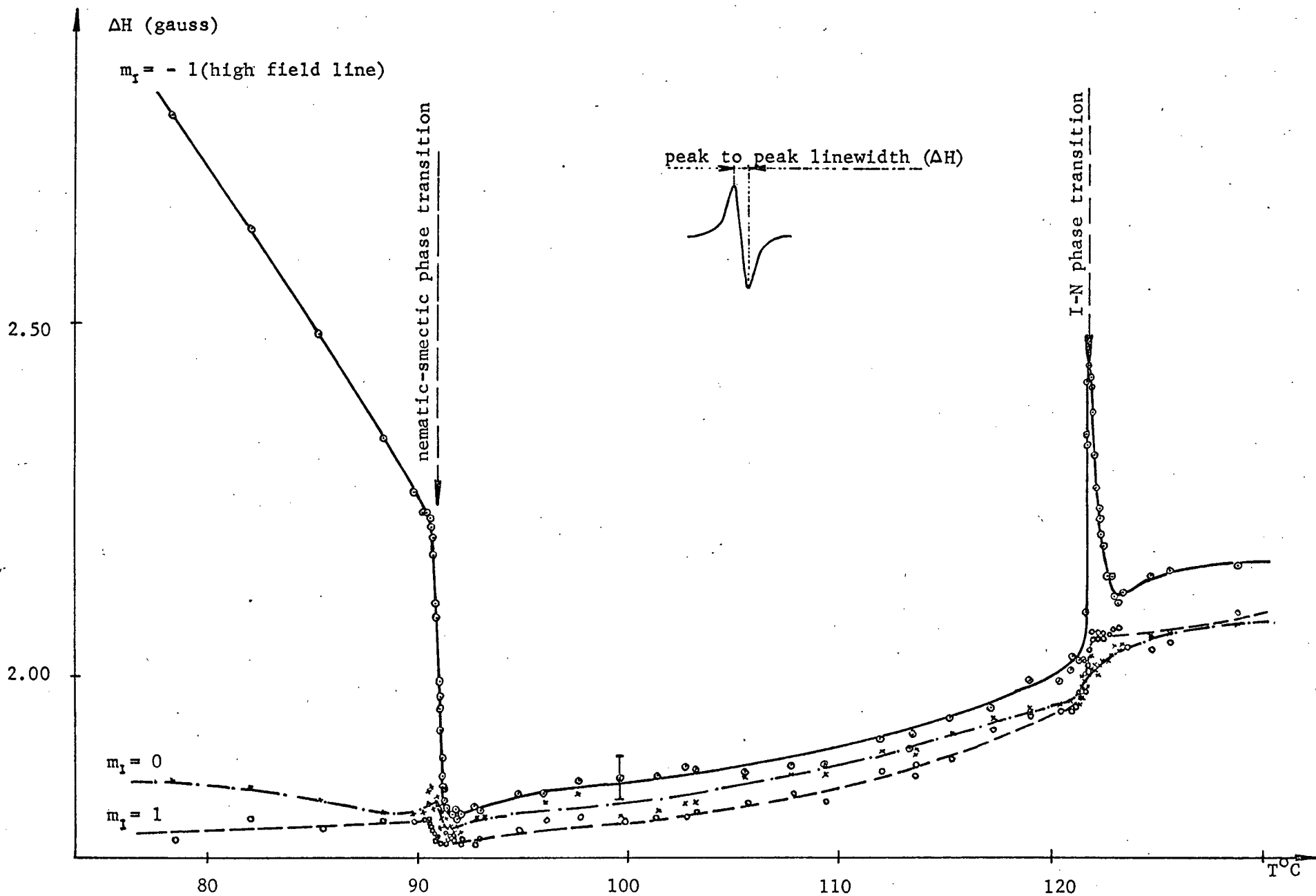


FIGURE 9.1

The peak to peak linewidths of the SL103 probe dissolved in HOAB as a function of the temperature.

linewidth for all three lines with decreasing temperature (increasing viscosity). This clearly shows that the ordering of the liquid crystal molecules affects the motions of a solute molecule. The linewidth of the high magnetic field line changes again at the nematic-smectic phase transition and then increases linearly with further decrease of the temperature. At this time, no detailed theoretical explanation has been proposed for the EPR linewidth anomalies near the phase transitions.

9.2 THE WIDTHS OF THE ABSORPTION LINES OF THE SYSTEM HOAB + VACA

The experimental errors of the linewidths of the system HOAB + SL103 are large since lines are only about two gauss wide. Since the ordering of the VACA molecules by the HOAB molecules is comparable to the ordering of the pure HOAB molecules, and because the VACA lines are much wider than those of SL103, we decided to study the system HOAB + VACA in detail. The relative experimental errors for this system are much smaller than for the system HOAB + SL103. The spectrum of the VACA dissolved in the low viscosity liquids consists of eight absorption lines and integrated intensities of the lines are approximately equal⁶⁶. An interesting feature of the VACA spectrum was first noted by Pake and Sands⁶⁷. They observed that the widths of the individual lines are proportional to the nuclear quantum number m_I . McConnell⁶⁸ first proposed a model in which the short range order produces a "microcrystal" about each VACA ion thus giving rise to anisotropies in the g-tensor and in the hyperfine interaction tensor. Roger and Pake⁶⁶ compared the linewidths of the VACA in aqueous solution measured at two microwave frequencies. Their results

confirmed the microcrystal model.

Since the width of the high magnetic field line is very broad and overlaps, we were not able to make a proper measurement of the linewidth of the highest field line, so that only seven lines were measured. Results of our measurements in the isotropic and nematic phase are shown in Figure 9.2a,b. From these two figures we conclude that, except for very close to the phase transition temperatures, the nuclear quantum number dependence of the linewidths is the same in both phases. This may mean that if a microcrystal is formed around the VACA ion in the isotropic liquid, it will remain present in the liquid crystal phase too. These figures show large increases in the linewidths at the I-N transition. It is clear that lines in the middle of the VACA spectrum change less than lines at the ends of the spectrum. This means that g-tensor fluctuations do not contribute as much as the fluctuations of the hyperfine tensor. In the nematic phase the linewidths decrease again. There are two reasons for the decrease of the linewidths in the nematic phase. One reason is that at the phase transition the viscosity of the nematic liquid crystal is lower than the viscosity of the same substance in the isotropic phase. The second reason is the molecular ordering of a liquid crystal. At a temperature below $\sim 100^{\circ}\text{C}$ the VACA linewidths start to increase again. The coefficients A, B, and C in the equation (8.1) were computed from the data in the Figure 9.2a,b. A computer program was used to solve the system of seven equations with three unknowns. To obtain the best values the least square fit was employed. These parameters are plotted as a function of the reduced temperature, T_R^* , in Figure 9.3.

Our calculations show that we may ignore the parameters

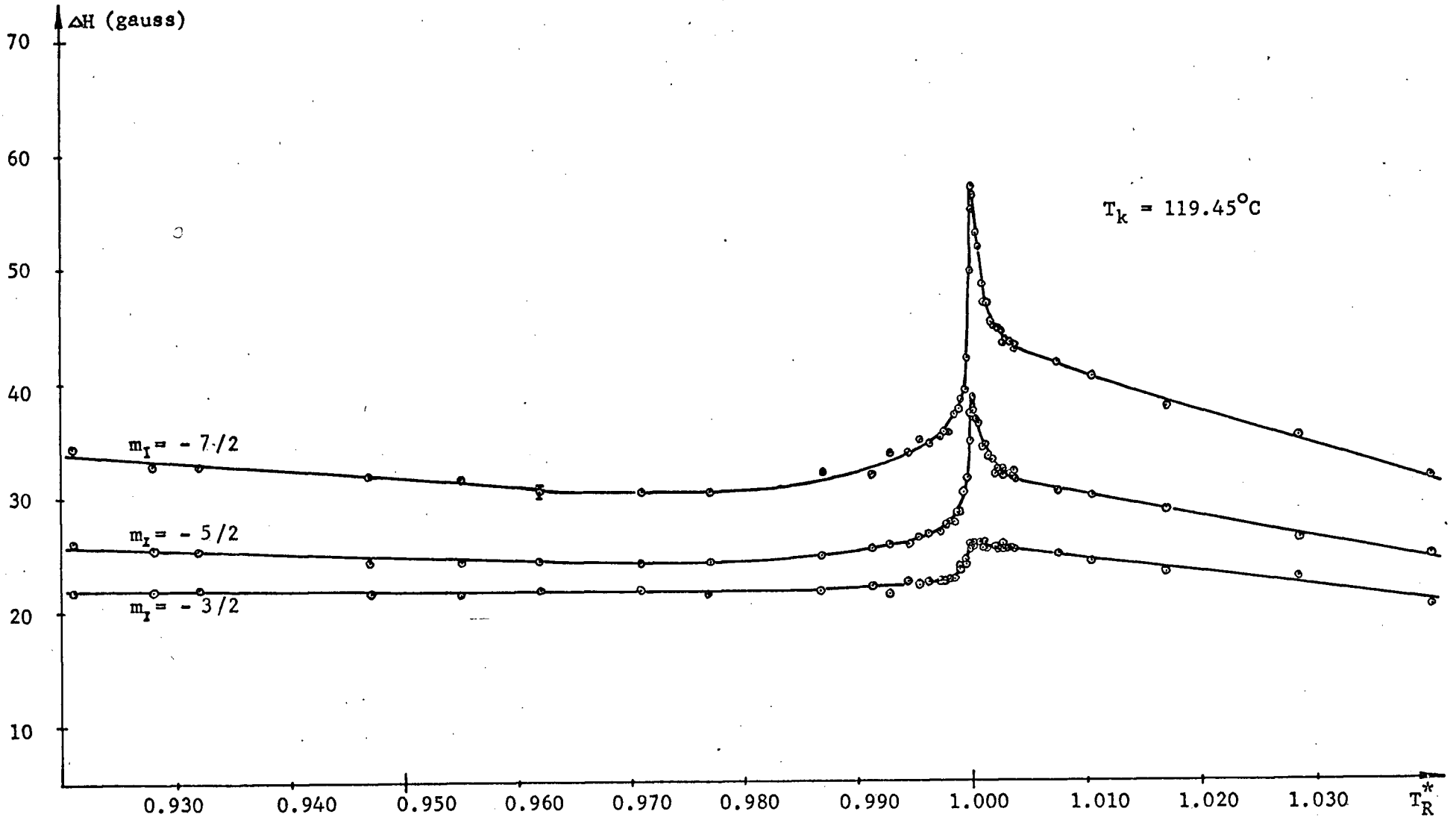


FIGURE 9.2a The peak to peak linewidths of the system HOAB + VACA as a function of the reduced temperature

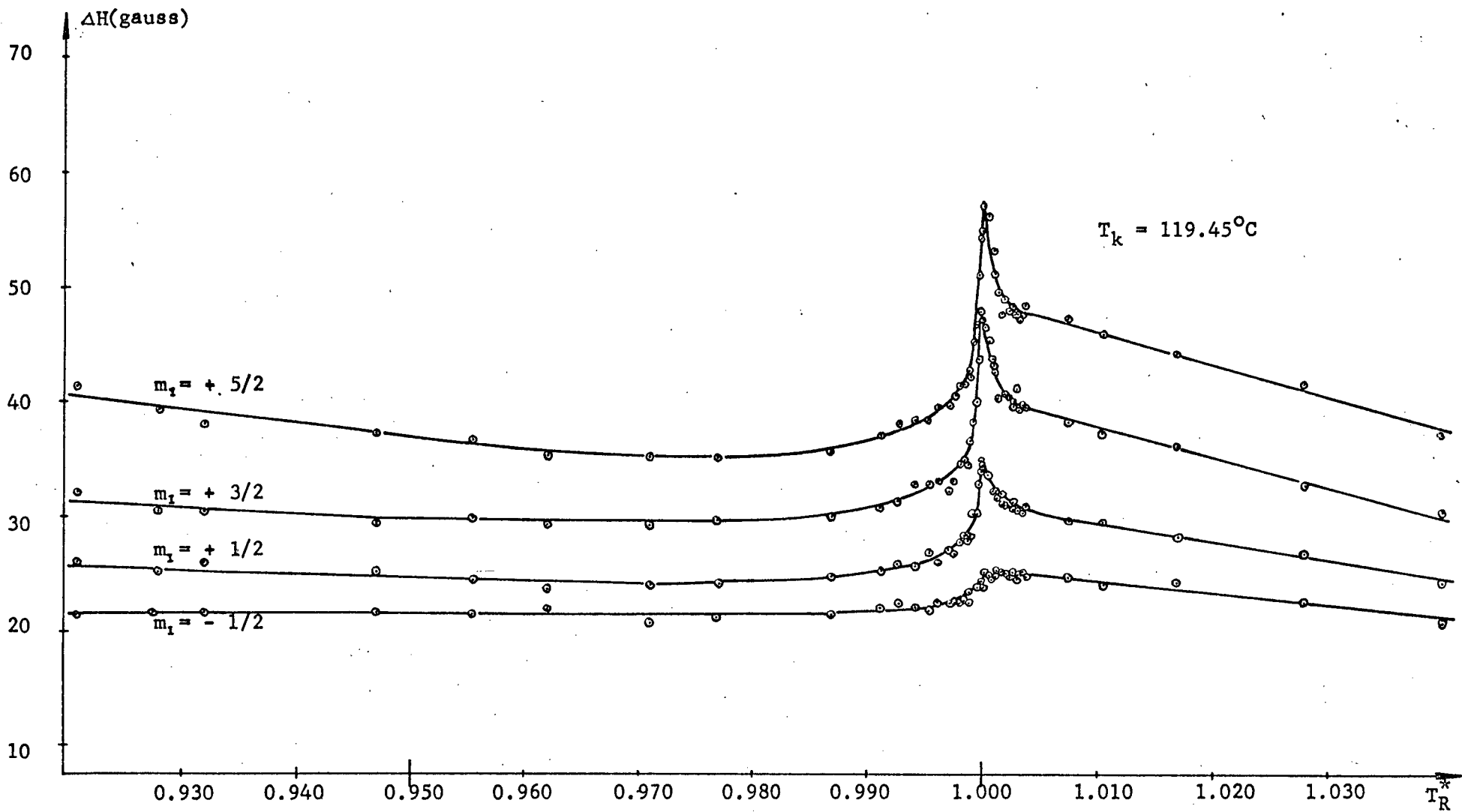


FIGURE 9.2b The peak to peak linewidths of the system HOAB + VACA as a function of the reduced temperature

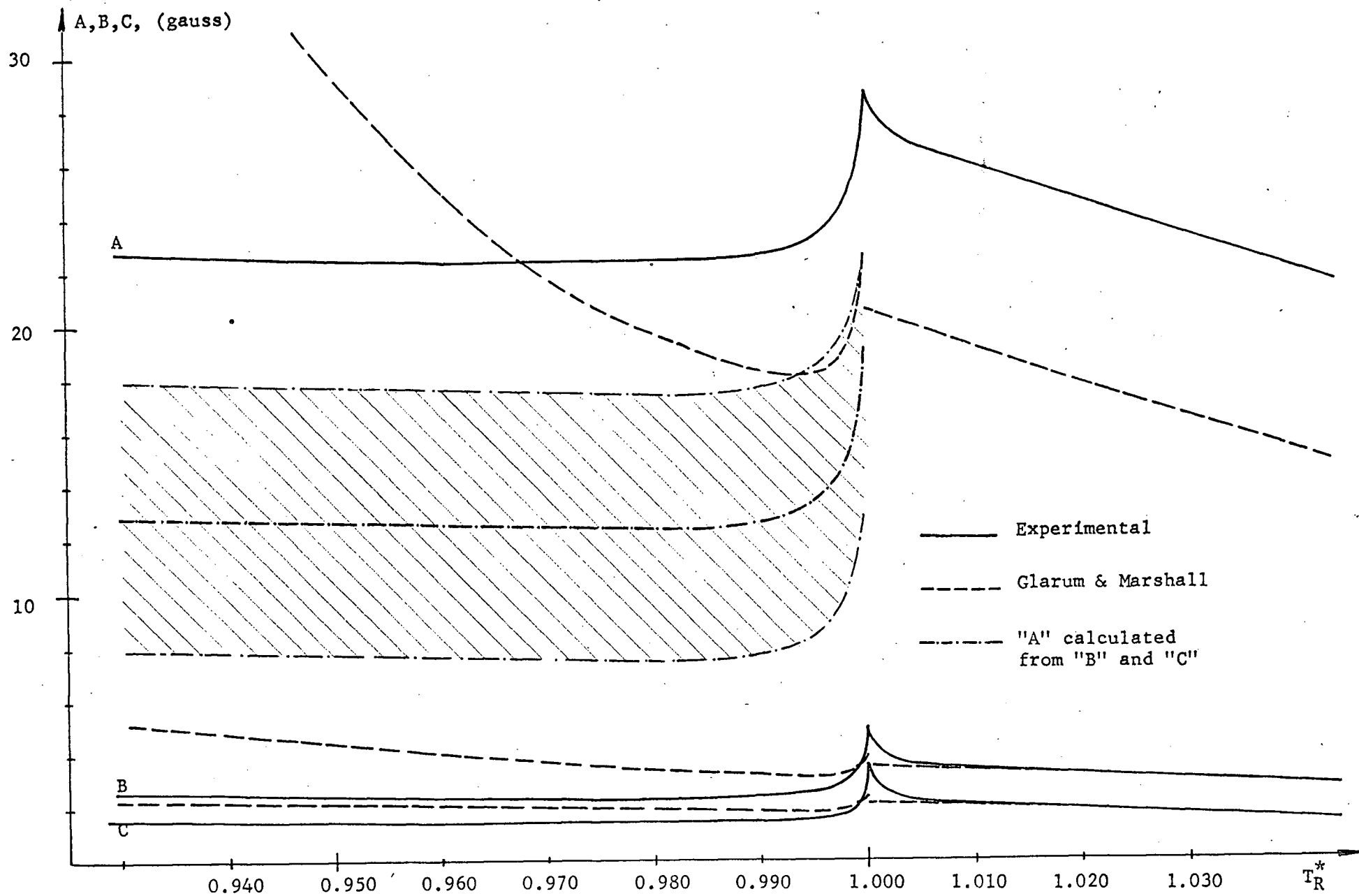


FIGURE 9.3 The coefficients A,B, and C from equation (8.1) as a function of the reduced temperature

involving " m_I^3 " and " m_I^4 " in equation (8.1) at temperatures far away from the I-N phase transition. However, very close to T_k equation (8.1) does not describe the line widths of the system HOAB + VACA correctly (see Appendix).

Doubts, regarding the increase of the linewidth at the I-N phase transition, might appear in a careful reader's mind. One might ask if the increase of the linewidth at the I-N phase transition is real or it is just an apparent effect due to the sample temperature fluctuations.

We estimated the fluctuations of the g-tensor at the I-N phase transition. Changes of the g-value as a function of the temperature could be calculated from equation (6.15). The temperature fluctuations in our experiments were less than $\pm 0.01^\circ\text{C}$. The estimated linewidth broadening arising from the g-value fluctuations did not exceed 0.1 gauss.

The temperature fluctuations and gradients change the positions of components of the total absorption line. From the temperature fluctuations in our experiment we estimated that the hyperfine splitting fluctuations "broaden" the VACA absorption line ($m_I = -7/2$) approximately 1 gauss. Since the total increase in the linewidth of the $m_I = -7/2$ line at the I-N phase transition was ~ 12 gauss, we believe, that the increase of the linewidths is a real effect (and not "an experimental effect" only).

CHAPTER 10

DISCUSSION10.1 ISOTROPIC PHASE OF THE SYSTEM HOAB + VACA

We assume that the isotropic phase of a liquid crystal allows the same type of motions of a solute molecule as an isotropic liquid of the same viscosity and which does not form a liquid crystal phase. The expressions (8.9) for A, B, and C are only approximations and more accurate formulae can be found in Wilson & Kivelson's paper⁴². They show that the coefficient C has to be used to calculate the hydrodynamic radius "r" (since the coefficient C is not dependent on spin-rotational relaxation and because it is linear in η/T). In the isotropic phase only the spectral densities at the frequency $\omega = 0$ are important. For this case

$$J_0(\omega=0) = J_1(\omega=0) = J_2(\omega=0) = \frac{2}{5} \tau_c \quad (10.1)$$

and τ_c is given by the equation (8.7). The value of the hydrodynamic radius which was calculated from the experimental results of Figure 9.3 at the reduced temperature $T_R^* = 1.040$ and $\eta/T = 10.6 \cdot 10^{-5} \frac{\text{stokes}}{^\circ\text{K}}$ is $r = 3.14 \cdot 10^{-8}$ cm. This value is consistent with the values obtained from isotropic liquids which do not form liquid crystal phases. In general, the values of the hydrodynamic radius for VACA dissolved in different isotropic liquids⁴⁴ are between 3.0 and 3.5 Å. The theoretical value of the ratio B/C obtained from equation (8.9) agrees well with the experimental one over most of the temperature range of the isotropic phase. In

Figure 9.3 we can see that the theoretical curves do not agree with the experimental ones very close to the I-N phase transition.

In the same way we calculated the theoretical values of the ratio A/C. We find that the theoretical values do not agree with the measured ones. The difference between the measured and calculated A using equation (8.9) and the measured values for the isotropic phase of the HOAB is about 7 gauss. Similar disagreements between the theoretical and experimental values A/C have been explained^{69,70} by taking into account spin-rotational interaction. According to Atkins & Kivelson, the spin-rotational interactions broadens the linewidth of an absorption line (as defined by equation (8.2)) of a free radical with axial symmetry which is dissolved in the isotropic liquid by an amount

$$\Delta H(\text{gauss}) = \frac{2\hbar}{\sqrt{3} g \beta_e} \frac{k}{12 \pi r^3} (\Delta g_{\parallel}^2 + 2\Delta g_{\perp}^2) \frac{T}{\eta} \quad (10.2)$$

where

$$\Delta g_{\parallel} = g_{\parallel} - 2.0023$$

$$\Delta g_{\perp} = g_{\perp} - 2.0023$$

In our case this contribution to the total linewidth is only 0.3 gauss at $T_R^* = 1.040$ and only about 0.2 gauss at $T_R^* = 1.000$. Therefore, the spin rotational-interaction or at least the theoretical expression (10.2) does not account for the disagreement of the constant A in our case.

The theoretical expressions for A, B, and C do not take into account effects which take place near the I-N phase transition temperature. Therefore one is led to a disagreement between the theory and experiment in this region. Our experiments show that very close to the I-N phase

transition temperature ($\Delta T < 2^\circ\text{C}$) the linewidths increase sharply for all lines except for the lines with $m_1 = -3/2$ and $m_1 = -1/2$. The maximum linewidth corresponds to the temperature at which the slope of the temperature dependence of the hyperfine splitting is steepest. It should be noted that in Chapter 6, we have defined the I-N transition temperature as that corresponding to the linewidth maximum.

As in Chapter 6 we explain the increase of the linewidths as being due to an increase in the correlation length associated with short range orientational order of small groups of the liquid crystal molecules. This causes small groups to become more and more interlocked with each other and such interlocking hinders their motions. The experimental measurements of the bulk viscosity (Figure 5.1) reveal no anomaly as the temperature is decreased to T_k . However, our studies of the lineshapes of the EPR lines do show that close to the I-N phase transition the lineshapes cannot be described, as at higher temperatures, by a simple Lorentzian. The computer fits indicated that the EPR spectrum of the VACA, as one approaches closer than approximately 5°C to T_k , resembles a composite Lorentzian and Gaussian form. This suggests that on the microscale the molecular motions are hindered as if the bulk viscosity were increased. Such an increase of the linewidth can, therefore, be explained by the slower motions of the small molecular groups as the I-N phase transition temperature is approached from above.

10.2 NEMATIC PHASE OF THE SYSTEM HOAB + VACA

Glarum & Marshall⁵ plotted the linear (B) and quadratic (C) coefficients from equations (8.4) as functions of the order parameter. They show that the linear coefficient decreases uniformly as the order parameter increases ($S \rightarrow 1.0$) and approaches zero asymptotically. Their study shows that the quadratic coefficient C vanishes too, but not in an asymptotic manner. When the order parameter S reaches 0.70 the coefficient C is equal to zero. With increasing order parameter it becomes negative and for complete order (at $S = 1.0$) it vanishes again.

Our experimentally determined coefficients A, B, and C are shown in Figure 9.3. The order parameter of the HOAB as obtained from our measurements (Figure 7.9) never reaches 0.70. However, the results plotted in Figure 9.3 (curves B and C) indicate that coefficients B and C start to increase below the reduced temperature $T_R^* = 0.97$ again. At this temperature the order parameter of the HOAB is $S = 0.40$.

Using equations (8.10), the order parameter from our measurements, and the flow viscosity from Figure 5.1, we calculated the coefficients A, B, and C. Our results are shown in Figure 9.3 with the dashed curves. It is clear that A, B, and C are all in disagreement with our experiment. This is not surprising since the assumption of a single correlation time is surely not valid in liquid such as liquid crystals because of the highly anisotropic intermolecular potential. Therefore, expression (8.7) is not very useful when studying the molecular motions in liquid crystals.

We calculated the coefficient A in the isotropic phase of HOAB as a function of the temperature. We can do similar calculations

for A in the nematic phase if we first obtain the spectral densities $\mathcal{J}_0(\omega)$ and $\mathcal{J}_1(\omega)$ from the measured B and C. Results of such calculations are shown in Figure 9.3 by the dash-dot curve. The experimental curve and the calculated curve have the same temperature dependence, but the difference in their magnitudes is about 10 gauss at all temperatures in the nematic phase, which is three gauss more than the difference in the isotropic phase.

We believe that the dash-dot curve describes the temperature dependence of A correctly. Its actual magnitude has no meaning from our experiment since it may contain systematic experimental error as large as 40% of the plotted value. This is shown with the shaded area in Figure 9.3.

Our computer fits have shown that the absorption lines in the nematic phase are slightly asymmetric. As the temperature of the system decreases to the nematic-smectic phase transition temperature, the line asymmetry decreases and lines become more Lorentzian. Similar asymmetry of the VACA absorption lines (4,4-dimethoxyazoxybenzene was used as a solvent) has been observed⁴ previously. Such a line asymmetry has been explained⁴ in terms of the slow ($\omega \sim 10^6 \text{ Hz}$) modulation of the orientation of the director. Since this motion is very slow on the EPR scale, the observed spectrum is simply a weighted sum of spectra from each possible orientation of the director. This misalignment of the director causes the asymmetry and broadening of the absorption lines and might be partially responsible for the disagreement between the experimental and "theoretical" value of the linewidth of the VACA in the nematic phase of HOAB.

We had pointed out that the coefficients B and C in equation (8.1) should decrease to zero as the order parameter becomes large. Our experiments do not confirm this. The observed increase of these two coefficients is probably caused by the increasing viscosity with decreasing

temperature (below $T = 115^{\circ}\text{C}$) in the HOAB nematic phase. From Figures 5.1 and 7.9 we see that viscosity increases much faster with temperature than does the order parameter. To conclude this chapter a few words will be said about the spectral densities, which appear in equation (8.10) and (8.11). We notice that experimental errors are quite large. However, we do feel that the description of the decay of the correlation function of the liquid crystal motion by a single correlation time exponential function is not adequate. This was clearly manifested at the temperature close to the I-N phase transition. To understand the molecular organization in liquid crystals, we believe, more experiments with different liquid crystals and solutes have to be done.

10.3 CONCLUSION

Flow viscosities of the pure MBME and HOAB in the isotropic and anisotropic phases were measured for the first time.

The phase transition temperature of the mixture of the MBME + VACA in vacuum was determined as a function of time.

Studies of the VACA probe in the viscous nematic crystal MBME provide evidence that orientation of the VACA molecules is suppressed by the liquid crystal molecules.

It is shown in this work that the apparent hyperfine splitting of the VACA dissolved in the viscous nematic crystals may be affected by the high viscosity of the solvent.

We show that in some cases (high viscosity) more accurate results can be obtained by measuring the splitting between the third ($m_{\tau} = -3/2$) and fourth ($m_{\tau} = -1/2$) absorption peak than by measuring the

splitting between the first ($m_I = -7/2$) and eight ($m_I = 7/2$) peaks.

Our measurements show that the SL103 paramagnetic probe does not reveal the order parameter of the studied liquid crystals satisfactorily.

From the changes of the hyperfine splitting as a function of the temperature it is possible to conclude that ordering of the liquid crystal molecules starts before the actual phase transition temperature is reached. This is the first such observation using the EPR technique.

We systematically measured the changes of the widths of the absorption lines as a function of temperature. The decrease of the linewidth when going from the isotropic to the nematic phase is explained by:

- a) decrease of the liquid crystal viscosity at the I-N phase transition
- b) ordering of the liquid crystal molecules in the liquid crystal nematic phase.

The absorption lines close to the phase transition temperature T_k do not have the usual Lorentzian shape.

The correlation time of the liquid crystal molecules increases if the sample temperature approaches T_k from above (slowing of the molecular motions). This is explained by the interlocking of small molecular groups.

The parameters B and C in equation (8.1) of the system HOAB + VACA in the nematic phase do not behave as predicted by Glarum & Marshall and Nordio et al. This is due to the increase of the flow viscosity as the temperature is lowered.

EPR absorption lines of the VACA probe dissolved in HOAB are slightly asymmetric in the high temperature region of the nematic phase. This is shown to indicate a low frequency modulation of the orientation of the director. This "misalignment" decreases with decreasing temperature.

According to Saupe's theory the order parameter of all nematic liquid crystals at T_k is ~ 0.4 . Our measurements do not confirm this.

Measurements with different solvents and solutes indicate that the ratios φ_1/φ_2 are roughly constant for different nematic liquid crystals (φ_1 and φ_2 are the order parameters of different paramagnetic probes dissolved in the same liquid crystal).

Even when ordering of a paramagnetic probe dissolved in nematic liquid crystals is small the width of a resonance line may be affected by the liquid crystal motions at the I-N phase transition. The condition $|\mathcal{H}'(t)\tau_c|^2 \ll 1$ is not valid very close to the I-N phase transition for the system HOAB + VACA.

Changes of the linewidths at the I-N phase transition indicate that the liquid crystal motions modulate the g-value less than the hyperfine splitting constant.

APPENDIX

We have mentioned (Chapter 9, section 2) that equation (8.1) does not describe the linewidths of the system HOAB + VACA in the vicinity of the I-N phase transition temperature satisfactorily. To estimate the experimental errors of the parameters A, B, and C and to estimate the magnitude of the parameters involving the " m_I^3 " and " m_I^4 " terms in equation (8.1) we decided to make the following check.

If one supposes that the linewidth of an absorption line of a paramagnetic probe dissolved in a liquid crystal is given by

$$\Delta H(m_I) = A + Bm_I + Cm_I^2 + Dm_I^3 + Em_I^4 \quad (\text{A.1})$$

than one may define the following quantities

$$\Delta H_{m_I}^{(+)} = \frac{1}{2} (\Delta H_{m_I} + \Delta H_{-m_I}) \quad (\text{A.2})$$

and

$$\Delta H_{m_I}^{(-)} = \frac{1}{2} (\Delta H_{m_I} - \Delta H_{-m_I}) \quad (\text{A.3})$$

Using equations (A.1), (A.2), and (A.3) one obtains

$$\Delta H_{m_I}^{(+)} = A + Cm_I^2 + Em_I^4 \quad (\text{A.4})$$

and

$$\Delta H_{m_I}^{(-)} = B m_I + D m_I^3 \quad (\text{A.5})$$

From equation (A.4) one sees immediately that plotting of $\Delta H_{m_I}^{(+)} = \Delta H_{m_I}^{(+)} (m_I^2)$ gives a straight line only if one may ignore the term " $E m_I^4$ ". If a straight line is obtained, the same plot gives A and C (together with the experimental errors).

From equation (A.5) one sees that a plot of $\Delta H_{m_I}^{(-)} / m_I$ as a function of m_I^2 should give a straight line which yields the parameters B and D together with their experimental errors.

We plotted such graphs at several reduced temperatures and some of them are shown in figures A.1 to A.5. Our graphs always give straight lines and this means that we may ignore the " $E m_I^4$ " term within experimental error.

The second thing which can be observed from these graphs is that the parameter D is zero, within experimental error, over most of the measured temperature range. However, it is different from zero and negative in the vicinity of the I-N phase transition temperature. This clearly indicates that equation (8.1) does not describe the linewidth of a paramagnetic probe near T_k satisfactorily and it suggests that equation (A.1) may have to be used in this temperature region.

The experimental errors of the parameter D are large. Though an examination of the theory⁴⁸ for the parameter D

$$D = \frac{1}{4} b^2 \frac{a - \frac{1}{2} b \sigma}{\omega_0} (4\sigma - 3\sigma_0)$$

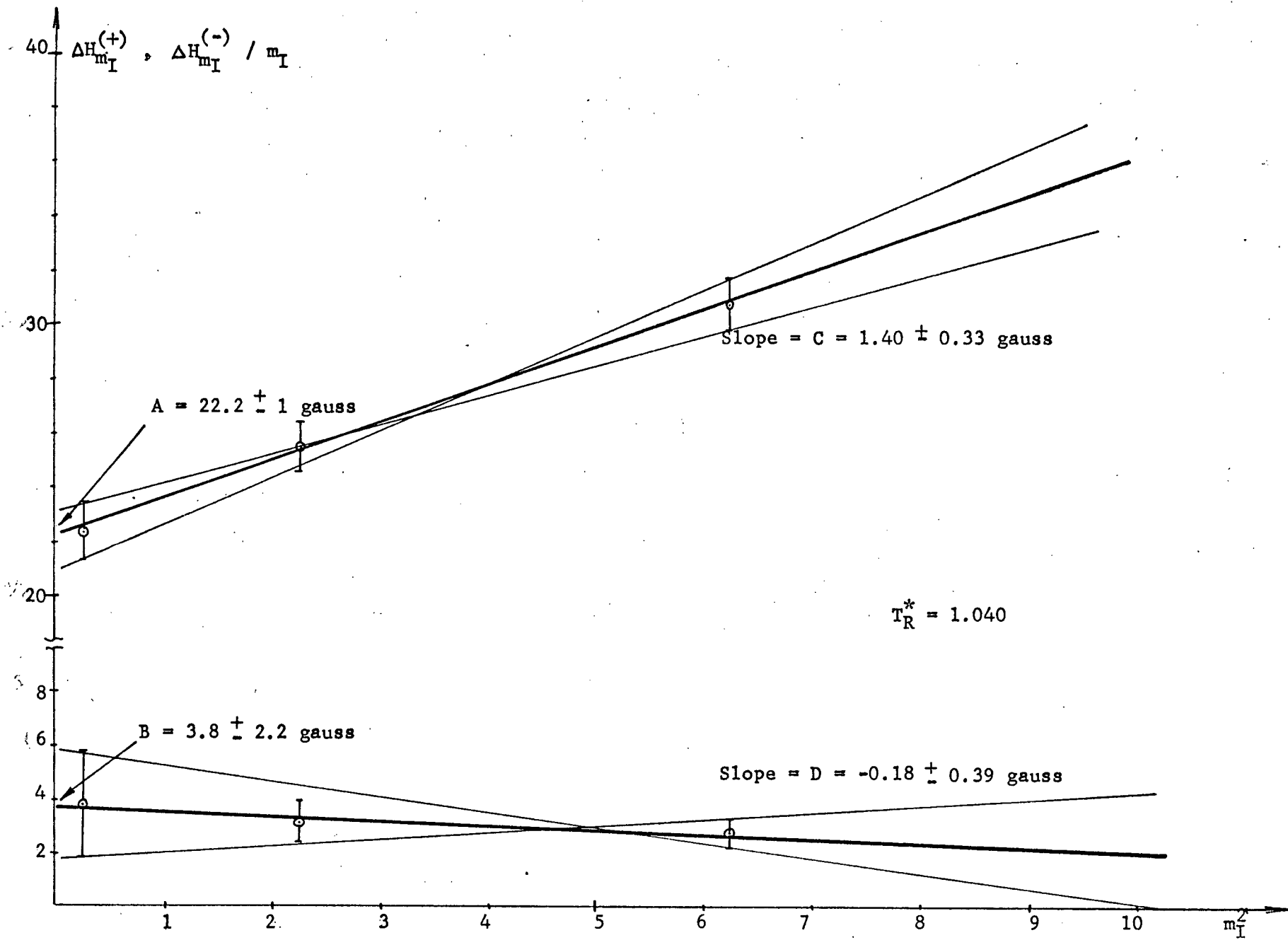


FIGURE A.1. $\Delta H_{m_I}^{(+)}$ and $\Delta H_{m_I}^{(-)}/m_I$ as functions of m_I^2

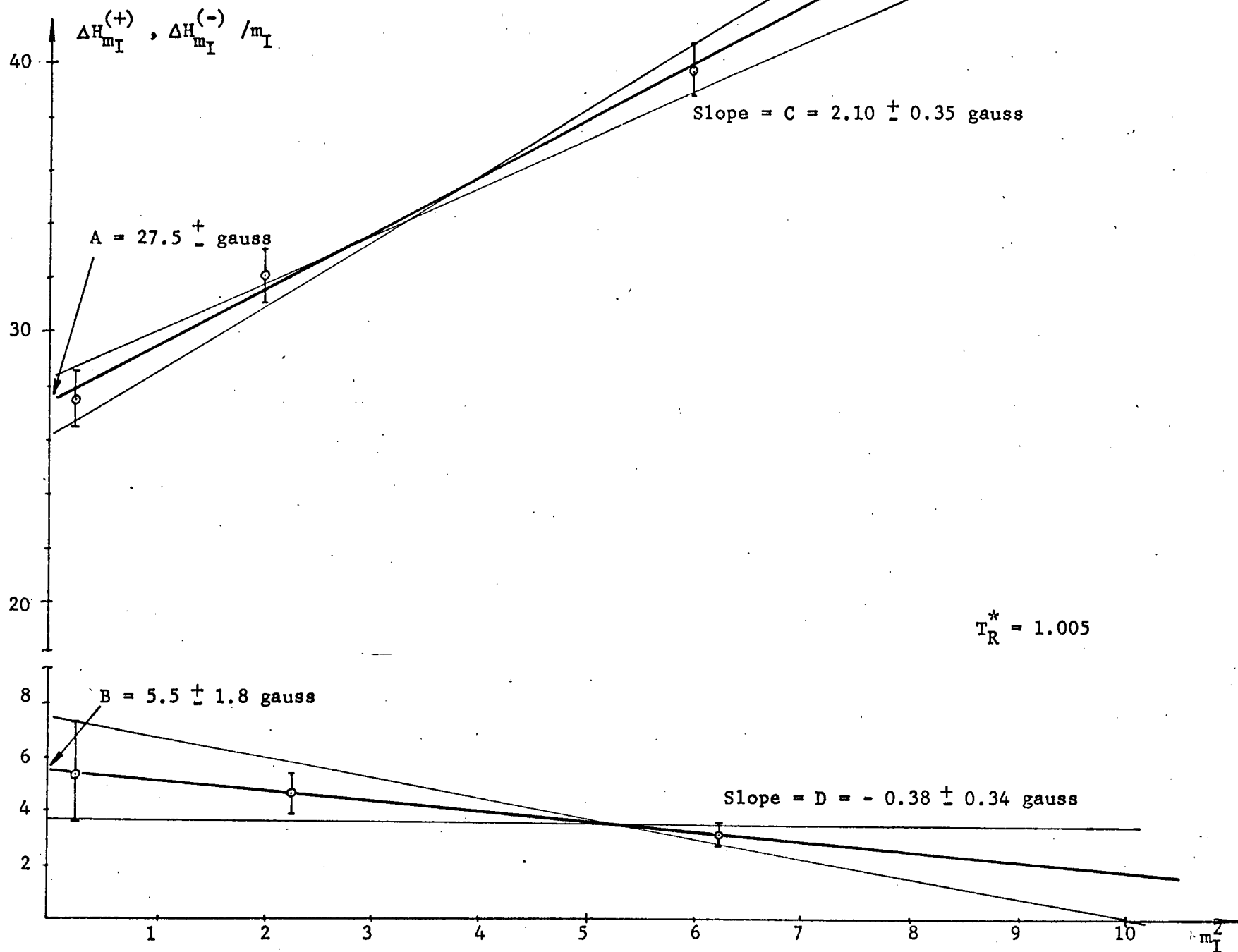


FIGURE A.2. $\Delta H_{m_I}^{(+)}$ and $\Delta H_{m_I}^{(-)} / m_I$ as functions of m_I^2

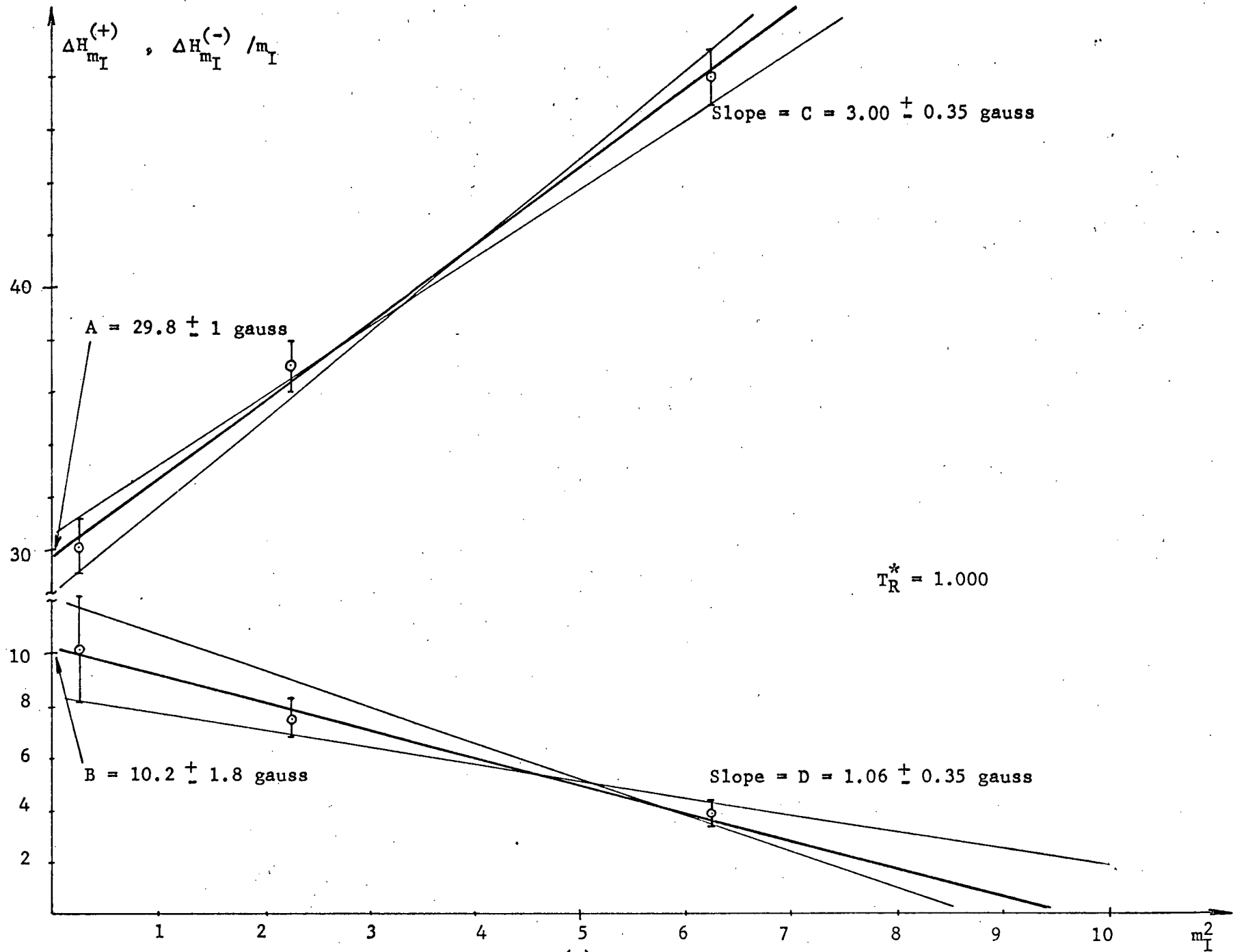


FIGURE A.3 $\Delta H_{m_I}^{(+)}$ and $\Delta H_{m_I}^{(-)} / m_I$ as functions of m_I^2

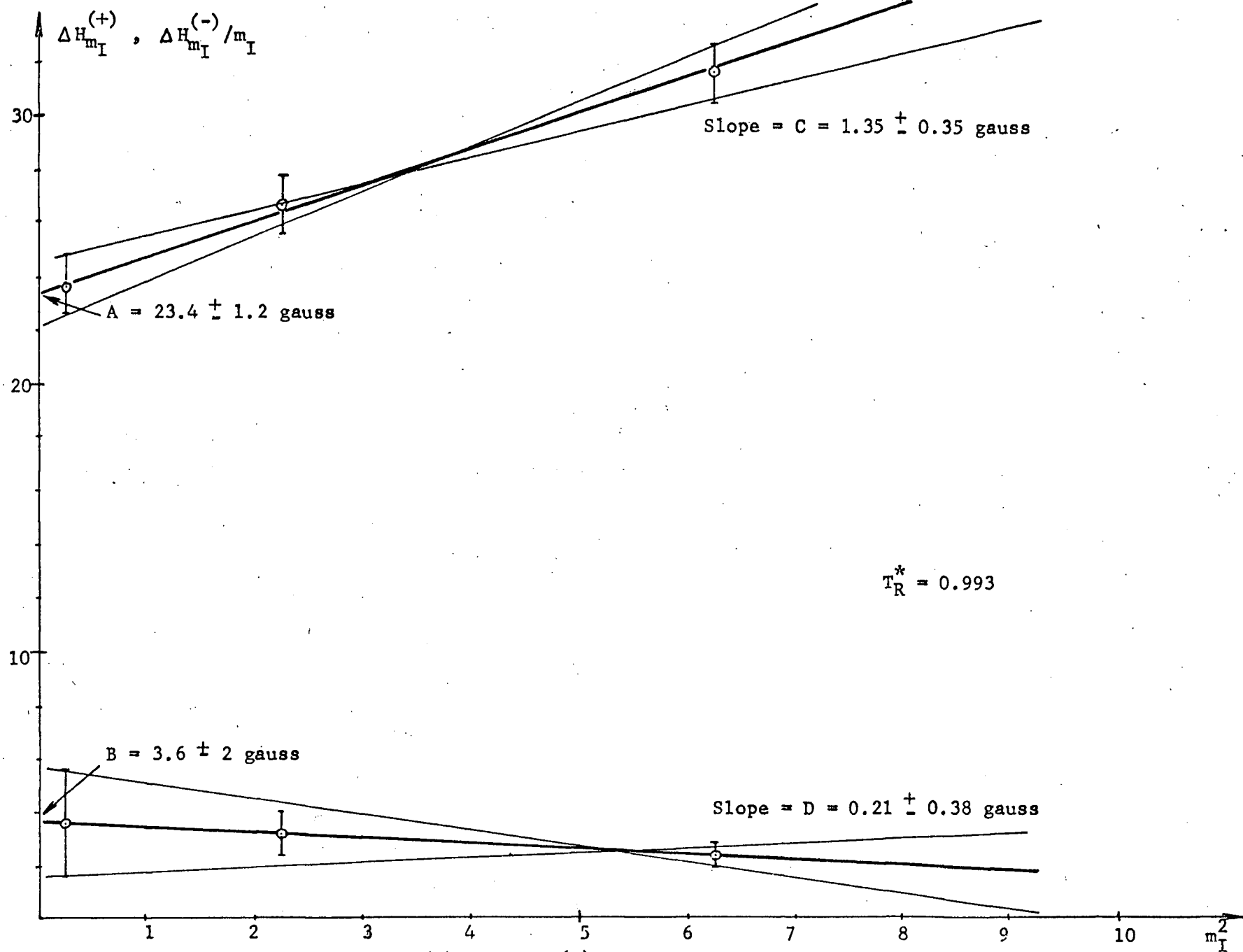
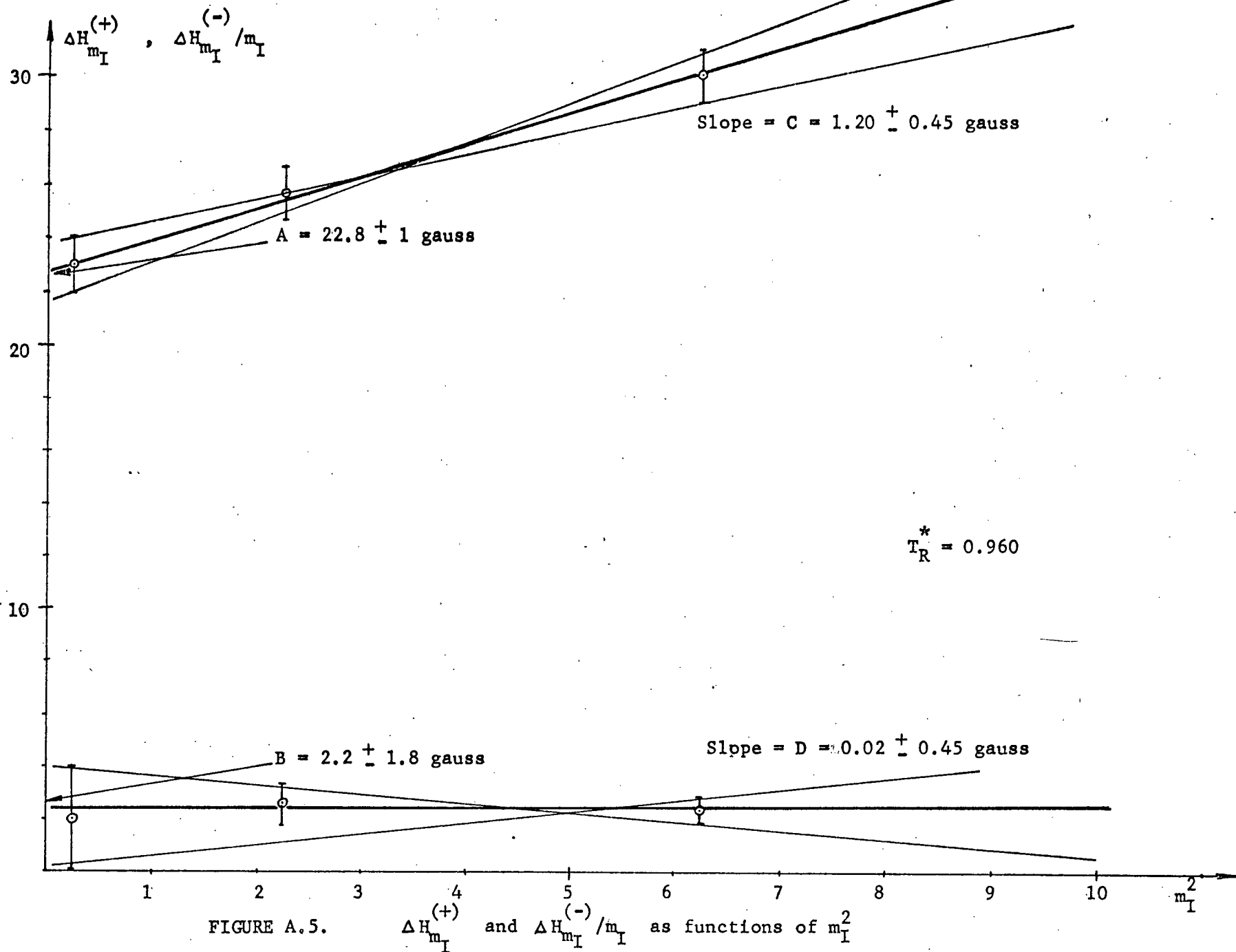


FIGURE A.4 $\Delta H_{m_I}^{(+)}$ and $\Delta H_{m_I}^{(-)} / m_I$ as functions of m_I^2



indicates that D is expected to be negative (as observed) and of order 3% of C , for our system, the present experiments are not definitive enough to provide a meaningful comparison of D with theory. However, this experiment clearly shows where more experiments are needed.

REFERENCES

1. Saupe, A., *Angew. Chem. - Inter. Edit.* 7, 97, (1968)
2. Cabane, B., *Adv. Mol. Relax. Processes* 3, 341 (1972)
3. Chen, D.H., Luckhurst G.R., *Trans. Farad. Soc.* 65, 656 (1969)
4. Brooks, S.A., Luckhurst, G.R., Pedulli, G.F. *Chem.Phys.Lett.* 11, 159 (1971)
5. Glarum, S.H., Marshall, J.H., *J. Chem. Phys.* 46, 55 (1967)
6. Nordio, P.L., Rigatti, G., Segre, U., *J. Chem. Phys.* 56, 2117 (1972)
7. Šentjarc, M., Schara, M., *Proc. Int. Liq.Cryst. Conf. 3rd Berlin* (1970)
8. Dong, R.Y., Marusic, M., Schwerdtfeger, C.F. *Sol.St. Comm.* 8, 1577 (1970)
9. Schwerdtfeger, C.F., Marusic, M., MacKay, A.L., Dong, R.Y., *Mol. Cryst. Liq. Cryst.* 12, 335 (1971)
10. Chistyakov, I.G., *Soviet Phys. - Uspekhi* 9, 551 (1967)
11. Brown, G.H., *Chemistry* 40, 10 (1969)
12. De Gennes, P.G., *Solid St. Comm.* 6, 163 (1968)
13. Brown, G.H., Doane, J.W., Neff, V.D., *Crit. Rev. Solid St. Sciences* 1, 303 (1970)
14. Luckhurst, G.R., *Phys. Bulletin* 23, 279 (1972)
15. De Gennes, P.G., *Mol. Cryst. Liq. Cryst.* 7, 325 (1969)
16. Sackmann, E., Meiboom, S., Snyder, L.C., *J. Am. Chem. Soc.* 89, 5981 (1967)
17. FRIEDEL, G., *Ann. Phys.* 18, 273 (1923)
18. Chistyakov, I.G., Vainshstein, B.K., *Soviet Phys. Cryst.* 8, 458 (1964)
19. Gelerinter, E., Fryburg, G.C., *Appl. Phys. Lett.* 18, 84 (1971)
20. Luckhurst, G.R., Sundholm, F., *Molec. Phys.* 21, 349 (1971)
21. Taylor, T.R., Ferguson, J.L., Arora, S.L., *Phys. Rev. Lett.* 24, 359 (1970)

22. Zocher, H., Phys. Z. 28, 790 (1927)
23. Frank, C.F., Disc. Farad. Soc. 25, 19 (1958)
24. Maier, W., Saupe, A., Z. Naturforsch 13a, 564 (1958)
25. Saupe, A., Z. Naturforsch 15a, 815 (1960)
26. Alben, R., Mol. Cryst. Liq. Cryst. 13, 193 (1971)
27. Hoyer, W.A., Nolle, A.W., J. Chem. Phys. 24, 803 (1956)
28. Kapustin, A.P., Zvereva, G.E., Soviet Phys.-Cryst. 10, 603 (1956)
29. Natale, G.G., Commins, D.E., Phys. Rev. Lett. 28, 1439 (1972)
30. Tsverkov, V.N., Ryumtsev E.I., Soviet Phys.- Cryst. 13, 225 (1968)
31. a) Litster, J.D., Stinson III, T.V., J. Appl. Phys. 41, 996 (1970)
b) Stinson III, T.V., Litster, J.D., Phys. Rev. Lett. 25, 503 (1970)
32. Pincus, P. Solid St. Comm. 7, 415 (1969)
33. Doane, J.W., Visintainer, J.J., Phys. Rev. Lett. 23, 1421 (1969)
34. Doane, J.W., Johnson, D.L., Chem. Phys. Lett. 6, 291 (1970)
35. Cabane, B., Clark, W.G., Phys. Rev. Lett. 25, 91 (1970)
36. Ghosh, S.K., Tettamanti, E., Indovina, P.L., Phys. Rev. Lett. 29, 638 (1972)
37. James, P.G., Luckhurst, G.R. Molec. Phys. 19, 439 (1970)
38. Porter, R.S., Barrall II, E.M., Johnson, J.F., J.Chem. Phys. 45, 1452 (1966)
39. Weber, K.H., Disc. Farad. Soc. 25, 74 (1958)
40. Ballhausen, C.J., Grayt, H.B., Inorg. Chem. 1, 111 (1961)
41. Kivelson, D., Sai-Kwing Lee, J. Chem. Phys. 41, 1896 (1964)
42. Wilson, R., Kivelson, D., J. Chem. Phys. 44, 154 (1966)
43. Fryburg, G.C., Gelerinter, E., J. Chem. Phys. 52, 3378 (1970)
44. Hudson, A., Luckhurst, G.R., Chem. Rev. 69, 191 (1969)
45. Spence, R.D., Gutowsky, H.S., Holm, C.H., J. Chem. Phys. 21, 1891 (1953)

46. Saupe, A., Englert, B., Phys. Rev. Lett. 11, 462 (1963)
47. Carrington, A., Luckhurst, G.R., Molec. Phys. 8, 401 (1964)
48. Luckhurst, G.R., Elec. Spin Relax. in Liquids (Edit. by L.T. Muus & P.W. Atkins 1972)
49. Rose, M.E., Element. Theory of Angular Momentum (John Wiley & Sons, New York, 1957)
50. Freed, J.H., Fraenkel, G.K., J. Chem. Phys. 39, 326 (1963)
51. Schwerdtfeger, C.F., Diehl, P., Molec. Phys. 17, 417 (1969)
52. Sands, R.H., Phys. Rev. 99, 1222 (1955)
53. Dodge, R.P., Tempelton, T.H., Zalkin, A., J. Chem. Phys. 35, 55 (1961)
54. Maier, W., Saupe, A., Z. Naturforsch. 15a, 287 (1960)
55. Glarum, S.H., Marshall, J.H., J. Chem. Phys. 44, 2884 (1966)
56. Atkins, P.W., Adv. Molec. Relax. Processes 2, 121 (1972)
57. Abragam, A., The Principles of Nuclear Resonance (Oxford Univ. Press, Oxford 1961)
58. Nordio, P.L., Busolin, P., J. Chem. Phys. 55, 5485 (1971)
59. Kivelson, D., J. Chem. Phys. 33, 1094 (1960)
60. Wilson, R., Kivelson, D., J. Chem. Phys. 44, 4445 (1966)
61. Orsay Liquid Crystal Group, J. Chem Phys. 51, 816 (1969)
62. Maier, W., Saupe, A., Z. Naturforsch 14a, 882 (1959)
63. James, P.G., Luckhurst, G.R., Molec. Phys. 19, 489 (1970)
64. Chandrasekhar, S., Krishnamurti, D., Madhusudana, N.V., Mol. Cryst. Liq. Cryst. 8, 45 (1969)
65. Nordio, P.L., Chem. Phys. Lett. 6, 250 (1970)
66. Rogers, R.N., Pake, G.E., J. Chem. Phys. 33, 1107 (1960)
67. Pake, G.E., Sands, R.H., Phys. Rev. 98A, 226 (1955)
68. McConnell, H.M., J. Chem. Phys. 25, 709 (1956)
69. Atkins, P.W., Kivelson, D., J. Chem. Phys. 44, 169 (1966)
70. Wilson, R., Kivelson, D., J. Chem. Phys. 44, 4440 (1966)
71. F.M. Leslie, G.R. Luckhurst, H.J. Smith: Chem. Phys. Lett. 13, 368, 1972.